Supporting Information for

Lithium fluoroarylsilylamides and their structural features

Sakshi Mohan, Yahya Al Ayi, Savarithai Jenani Louis Anandaraj,
Marie Cordier, Thierry Roisnel, Jean-François Carpentier, and Yann Sarazin*

Corresponding author: Yann Sarazin, Université de Rennes, CNRS, Institut des Sciences Chimiques de Rennes, UMR 6226, Campus de Beaulieu, 35042 Rennes Cedex France, e-mail: yann.sarazin@univ-rennes.fr

Sakshi Mohan, Yahya Al Ayi, Savarithai Jenani Louis Anandaraj, Marie Cordier, Thierry Roisnel and Jean-François Carpentier: Université de Rennes, CNRS, Institut des Sciences Chimiques de Rennes, UMR 6226, Campus de Beaulieu, 35042 Rennes Cedex France

Contents

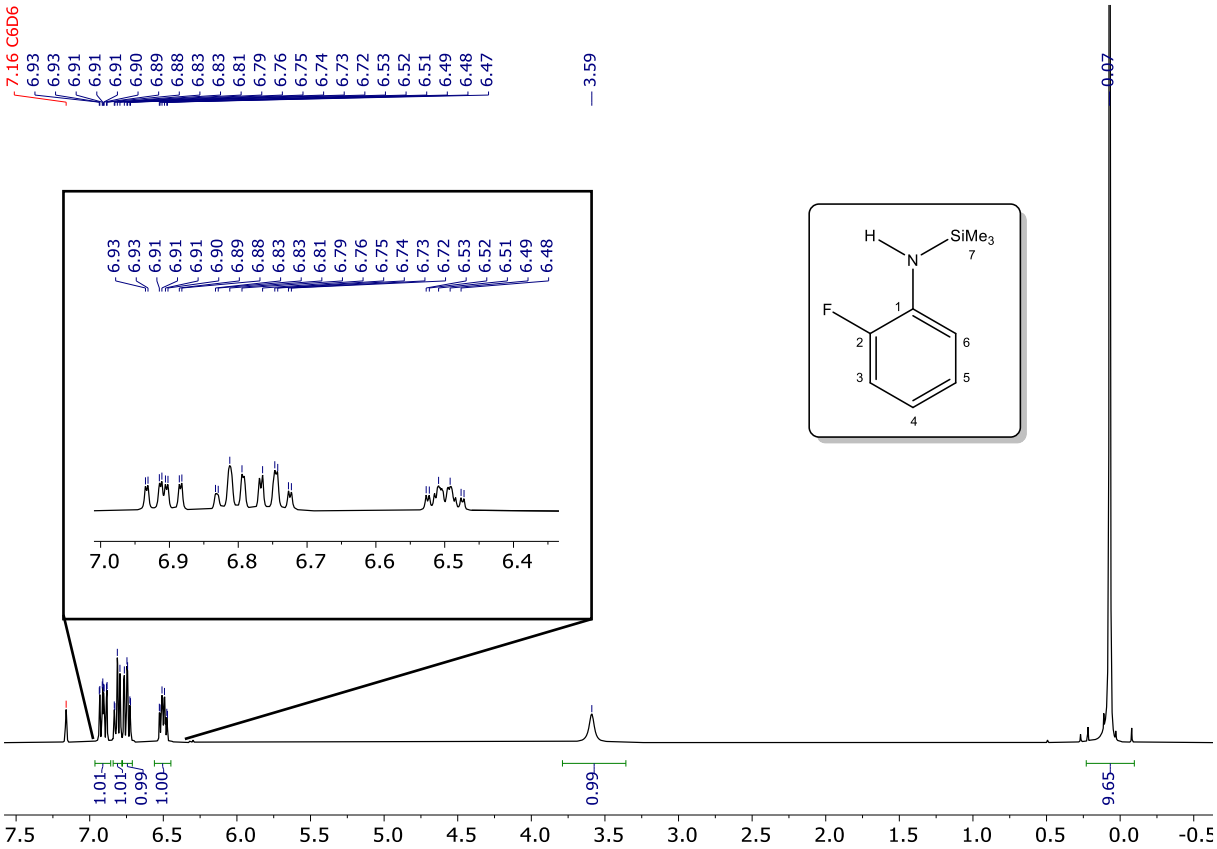

Fig. S1. ^{1}H NMR spectrum (benzene-d_6, 400.16 MHz, 27 °C) of *N*-(2-fluorophenyl)-trimethylsilylamine (**1-H**).

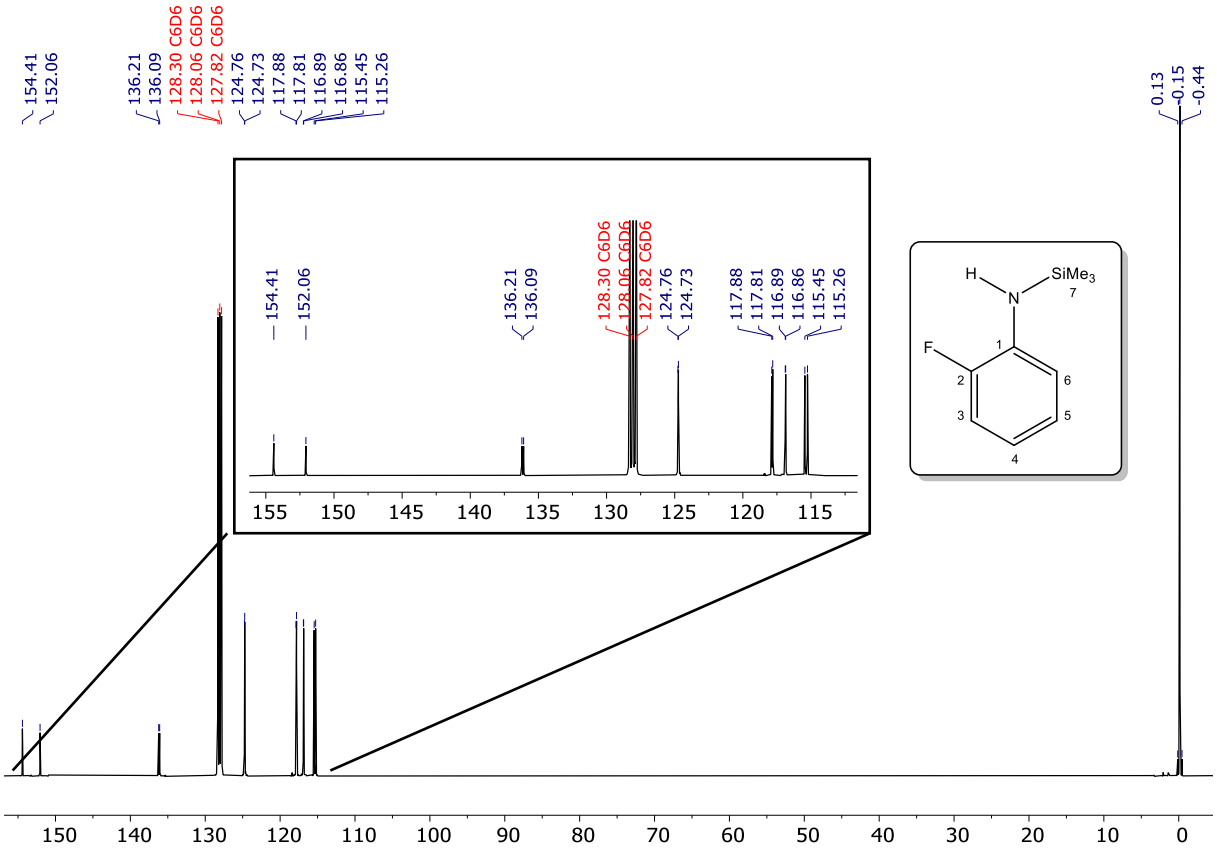

Fig. S2. $^{13}C\{^{1}H\}$ NMR (benzene-d_6, 100.63 MHz, 27 °C) of *N*-(2-fluorophenyl)-trimethylsilylamine (**1-H**).

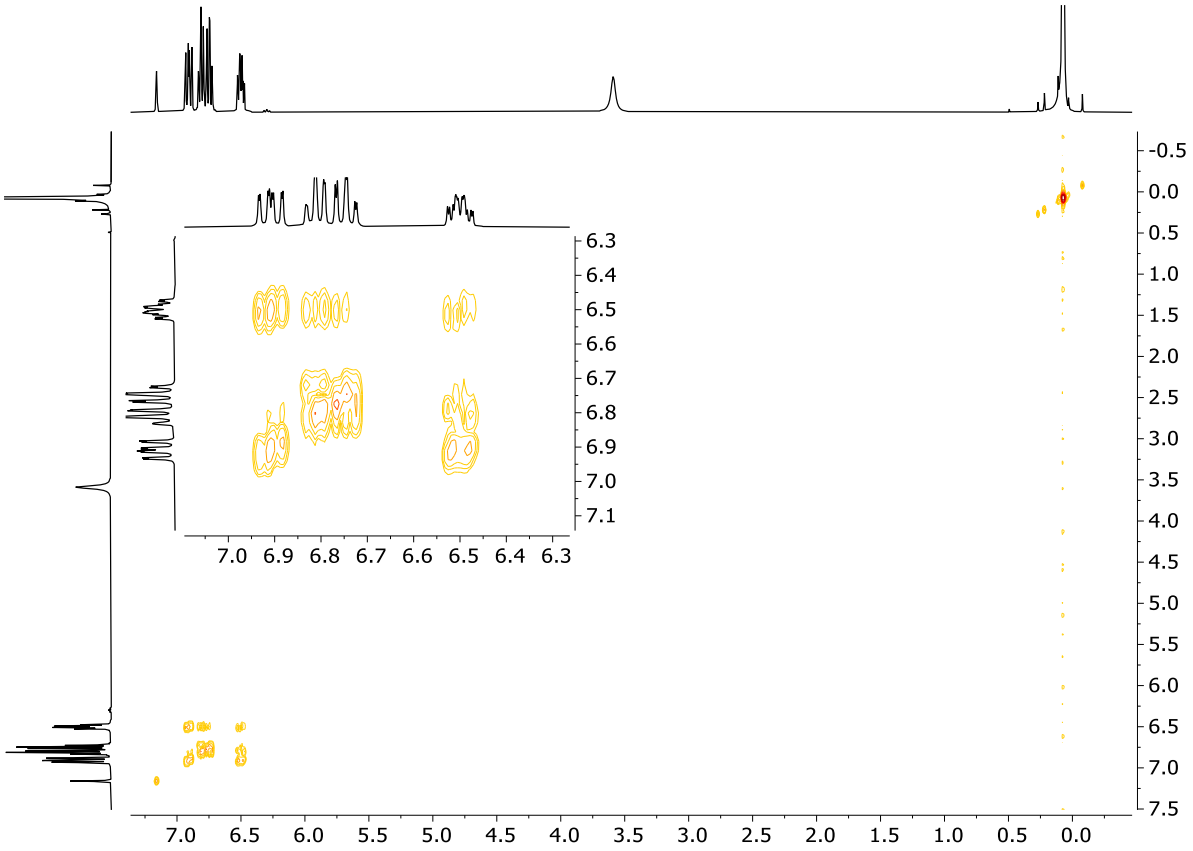

Fig. S3. COSY ^{1}H-^{1}H NMR (benzene-d_6, 400.16 MHz, 27 °C) of *N*-(2-fluorophenyl)-trimethylsilylamine (**1-H**).

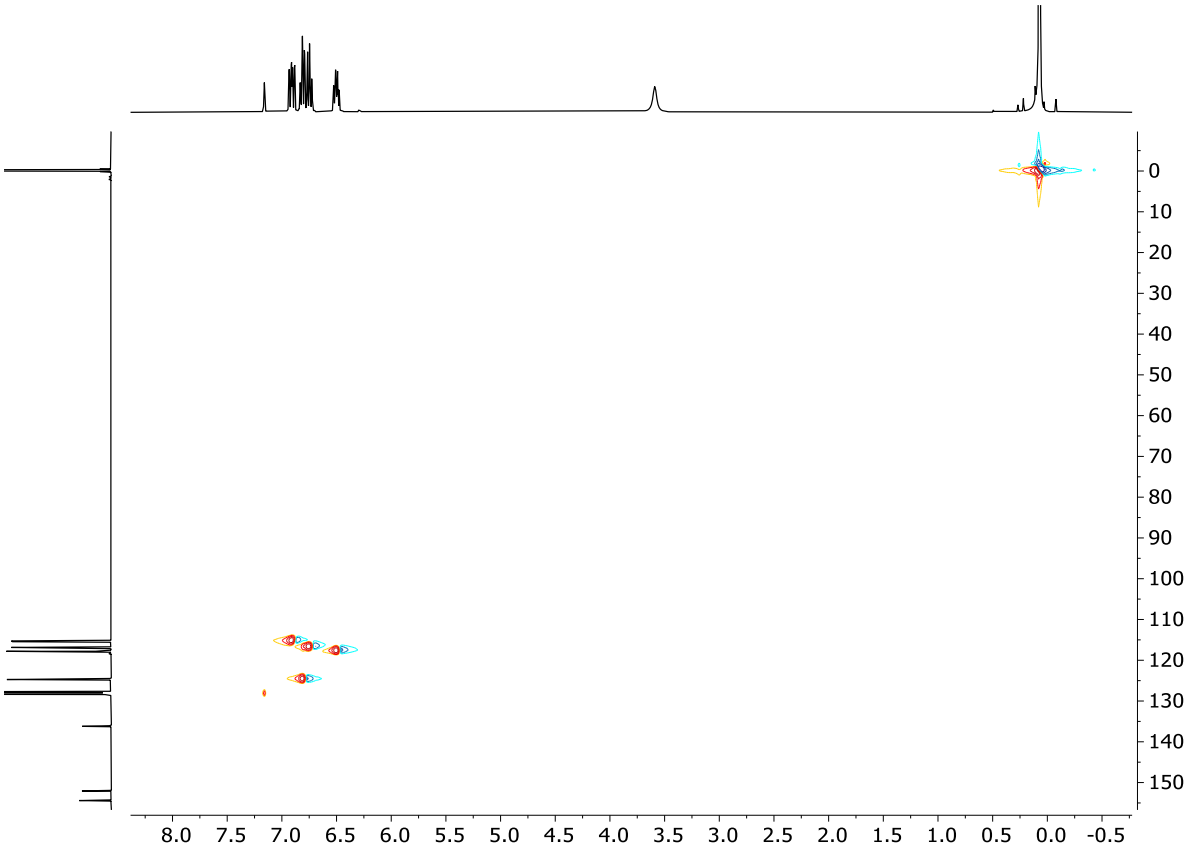

Fig. S4. HSQC ^{1}H-^{13}C NMR (benzene-d_6, 400.16/100.63 MHz, 27 °C) of *N*-(2-fluorophenyl)-trimethylsilylamine (**1-H**).

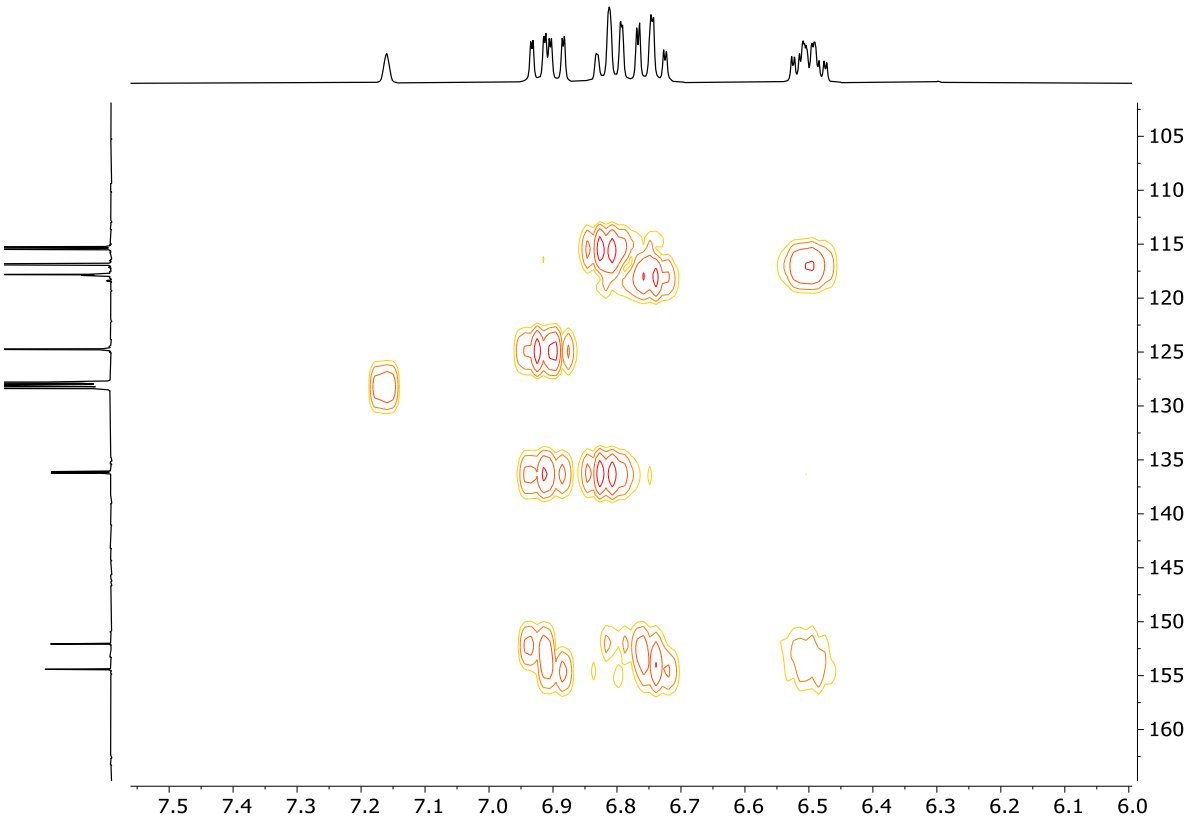

Fig. S5. HMBC ^{1}H-^{13}C NMR (benzene-d_6, 400.16/100.63 MHz, 27 °C) of *N*-(2-fluorophenyl)-trimethylsilylamine (**1-H**).

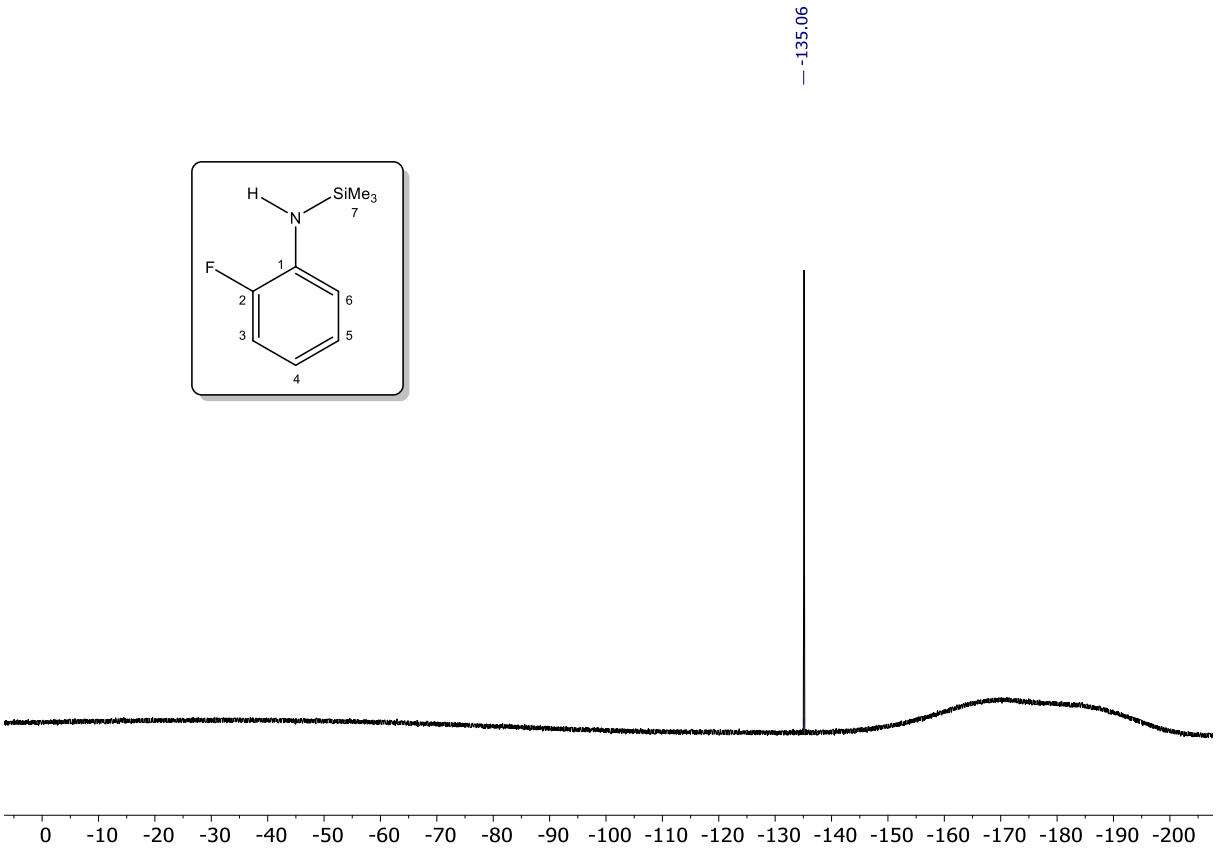

Fig. S6. ^{19}F NMR spectrum (benzene-d_6, 376.47 MHz, 25 °C) of *N*-(2-fluorophenyl)-trimethylsilylamine (**1-H**).

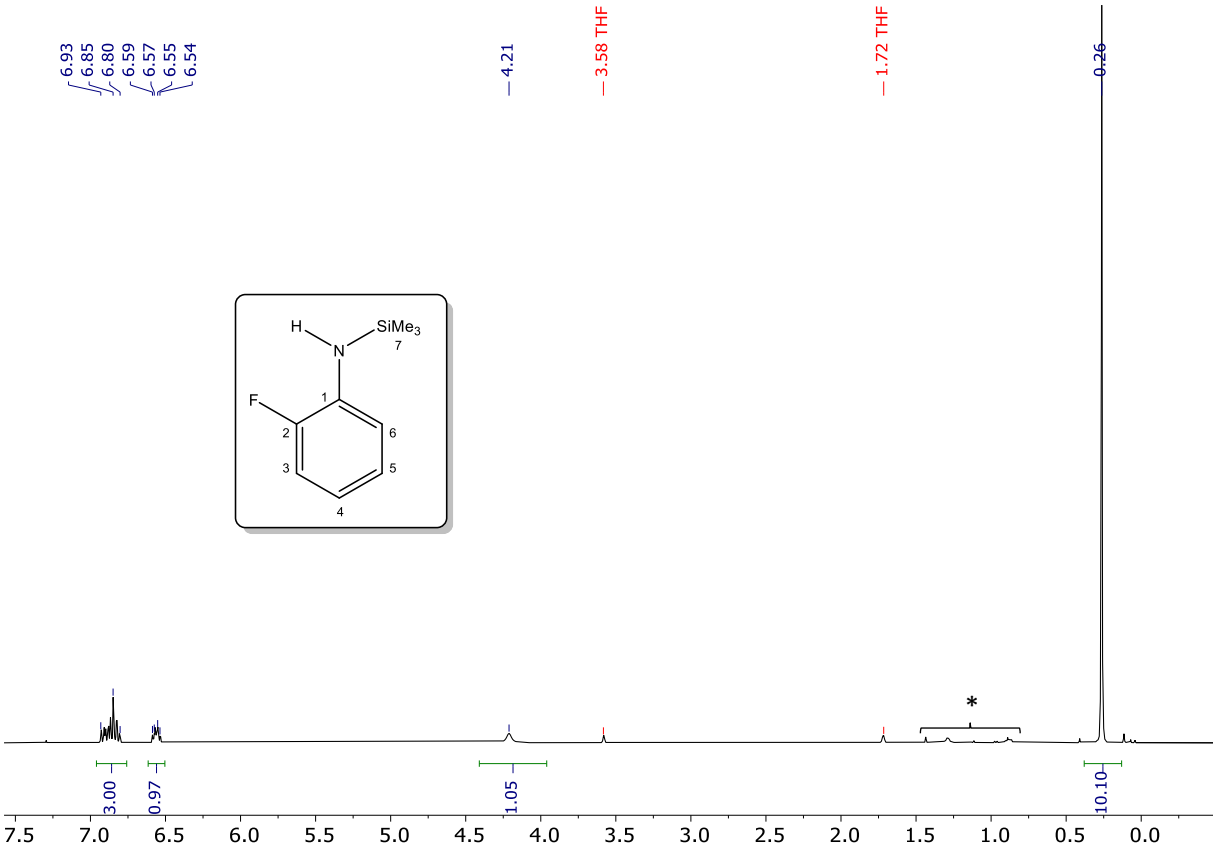

Fig. S7. ^{1}H NMR spectrum (thf-d_8, 400.16 MHz, 25 °C) of *N*-(2-fluorophenyl)- trimethylsilylamine (**1-H**). * = residual solvents (Et_2O and petroleum ether).

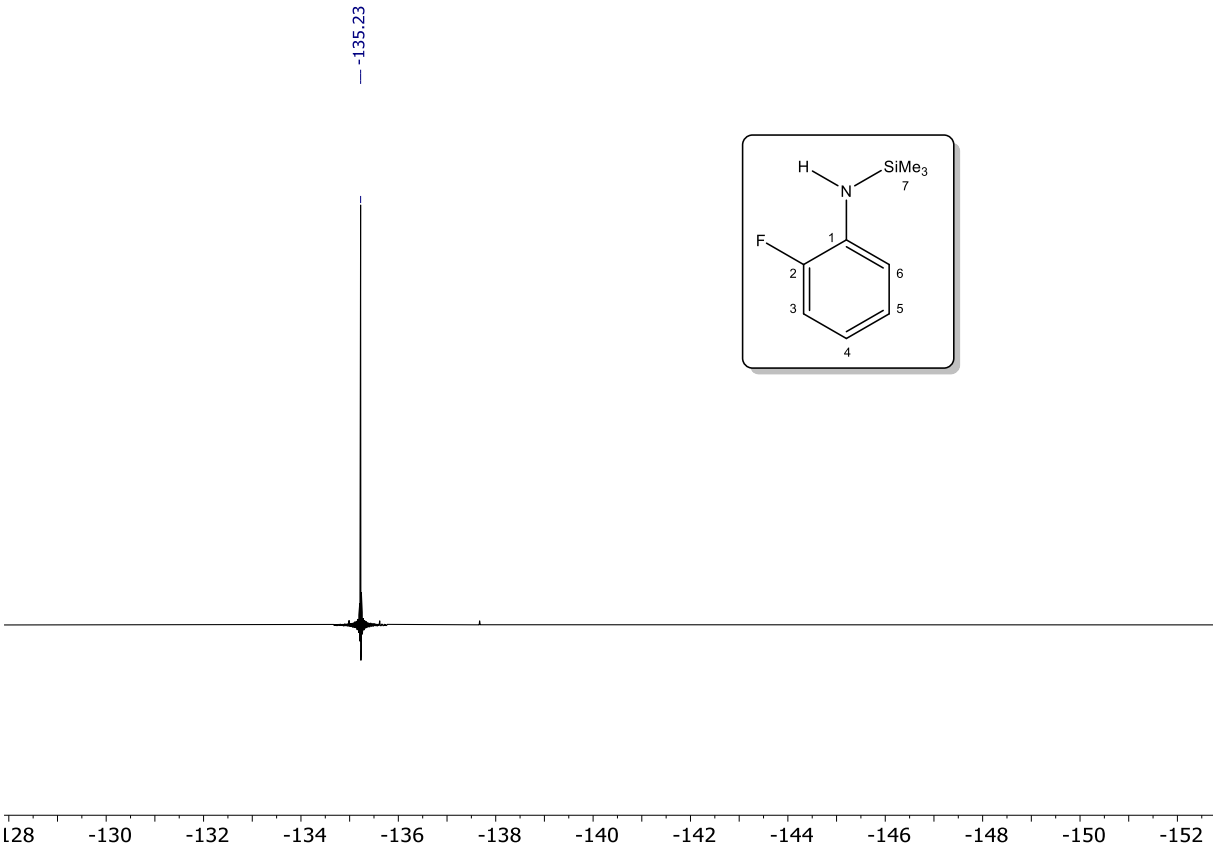

Fig. S8. ^{19}F NMR spectrum (thf-d_8, 376.47 MHz, 25 °C) of *N*-(2-fluorophenyl)-trimethylsilylamine (**1-H**).

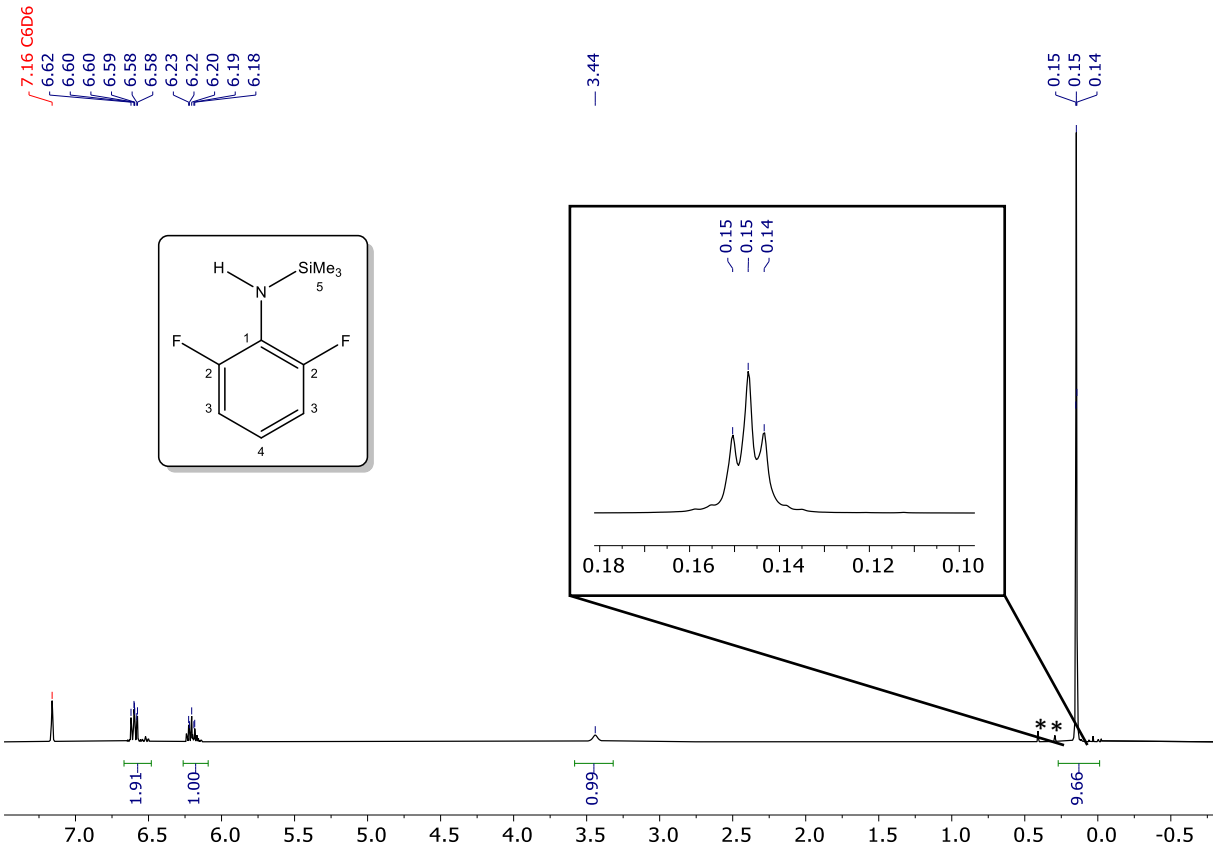

Fig. S9. ^{1}H NMR spectrum (benzene-d_6, 400.13 MHz, 24 °C) of *N*-(2,6-difluorophenyl)-trimethylsilylamine (**2-H**). * = residual impurities (water, 0.40 ppm, and silicone grease, 0.29 ppm).

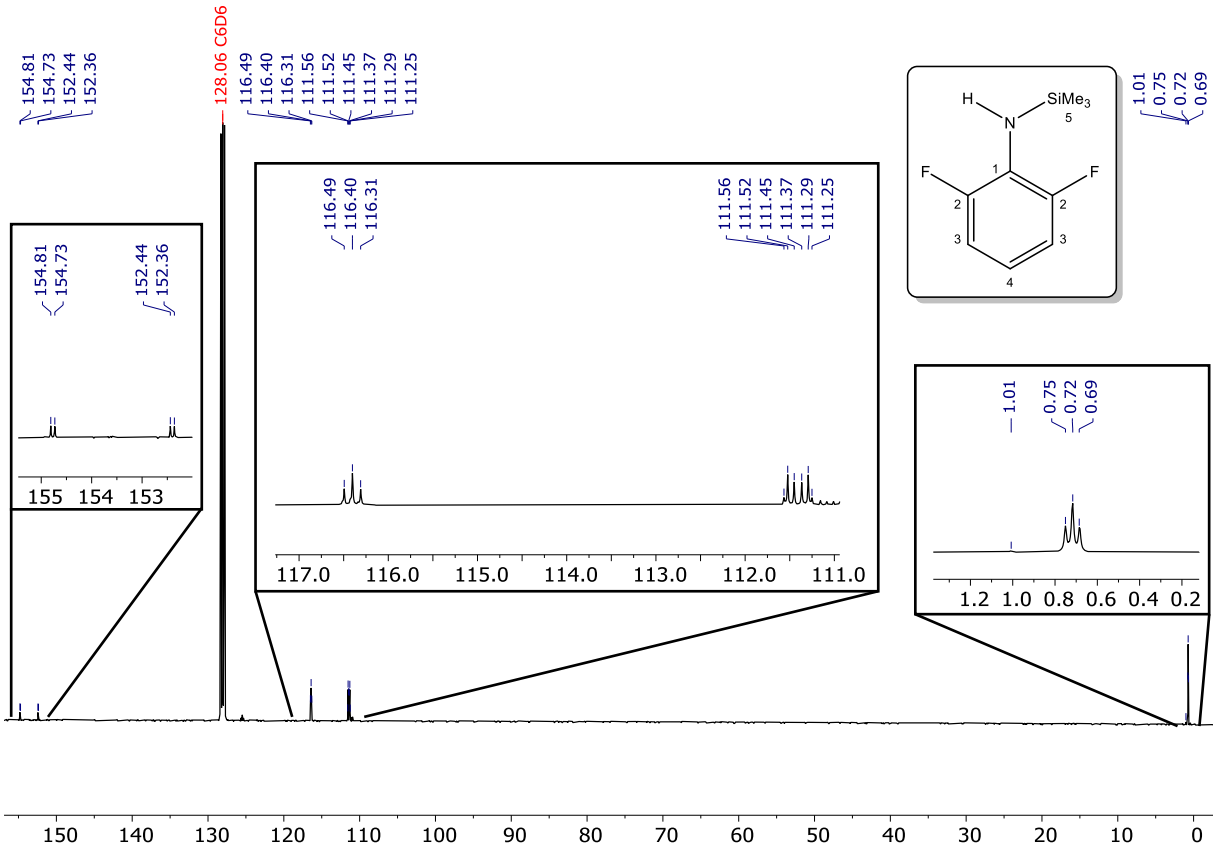

Fig. S10. $^{13}C\{^{1}H\}$ NMR spectrum (benzene-d_6, 100.62 MHz, 26 °C) of *N*-(2,6-difluorophenyl)-trimethylsilylamine (**2-H**). * = residual impurities (silicone grease, 1.01 ppm).

Fig. S11. ^{19}F NMR spectrum (benzene-d_6, 282.36 MHz, 25 °C) of *N*-(2,6-difluorophenyl)-trimethylsilylamine (**2-H**).

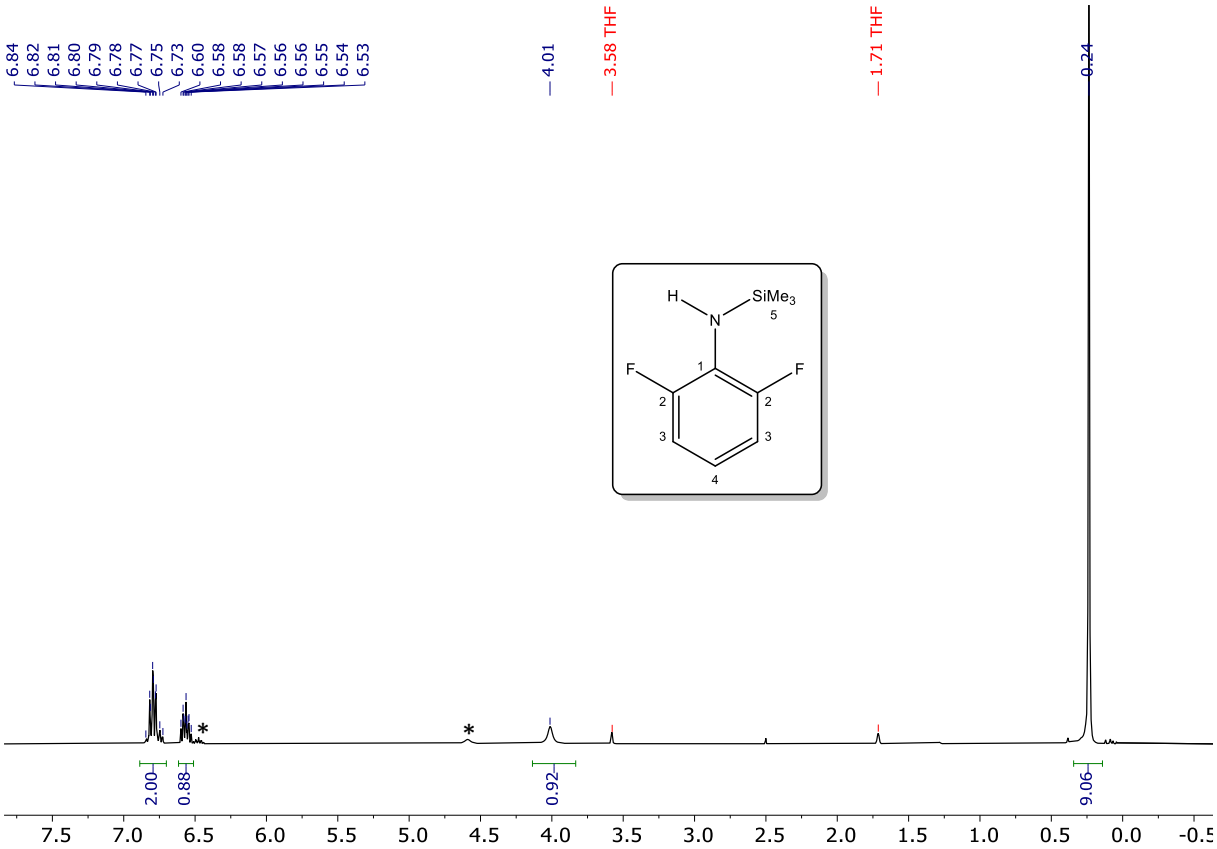

Fig. S12. ^{1}H NMR spectrum (thf-d_8, 400.16 MHz, 27 °C) of *N*-(2,6-difluorophenyl)-trimethylsilylamine (**2-H**). * = 2,6-F_2-C_6H_3-NH_2 resulting from hydrolysis during sample preparation.

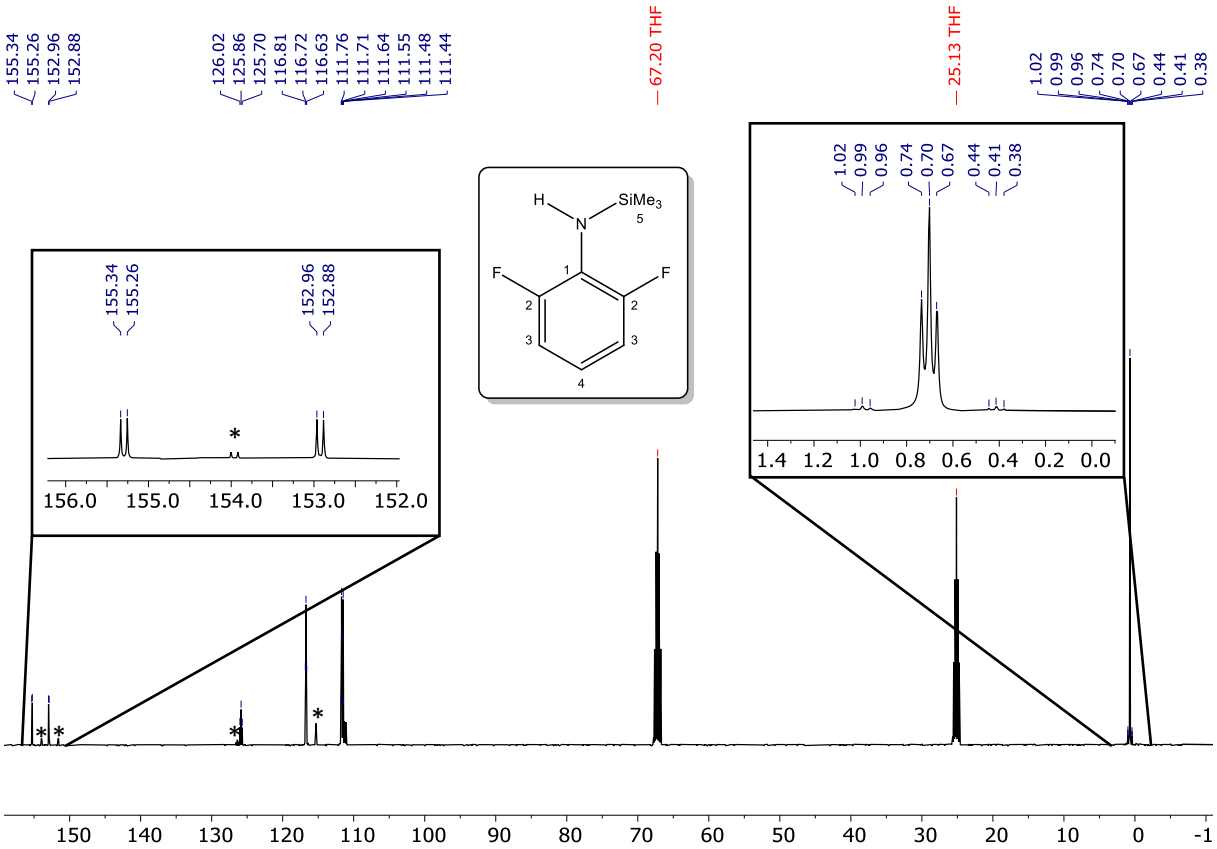

Fig. S13. $^{13}C\{^{1}H\}$ NMR spectrum (thf-d_8, 100.63 MHz, 27 °C) of *N*-(2,6-difluorophenyl)-trimethylsilylamine (**2-H**). * = 2,6-F_2-C_6H_3-NH_2 resulting from hydrolysis during sample preparation.

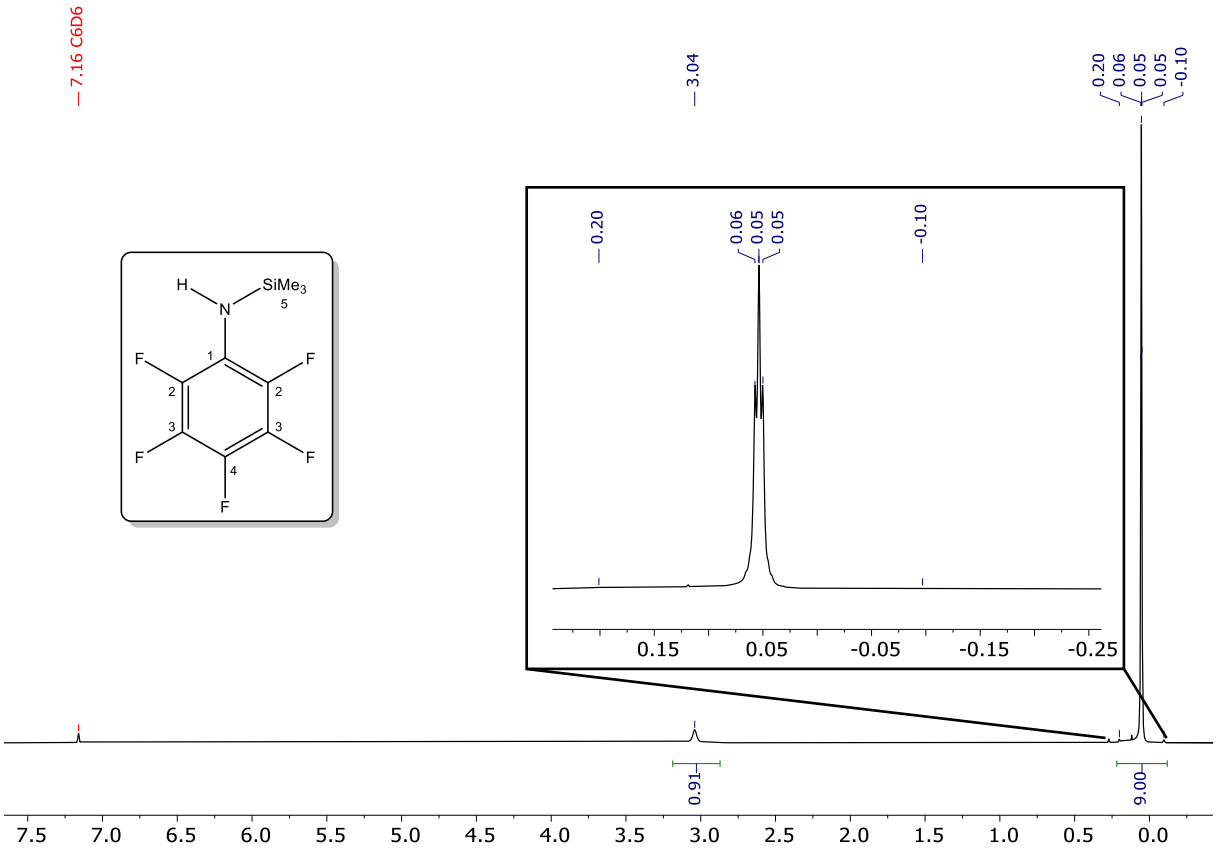

Fig. S14. ^{1}H NMR spectrum (benzene-d_6, 400.16 MHz, 27 °C) of *N*-(pentafluorophenyl)-trimethylsilylamine (**3-H**). * = residual solvents (water and petroleum ether).

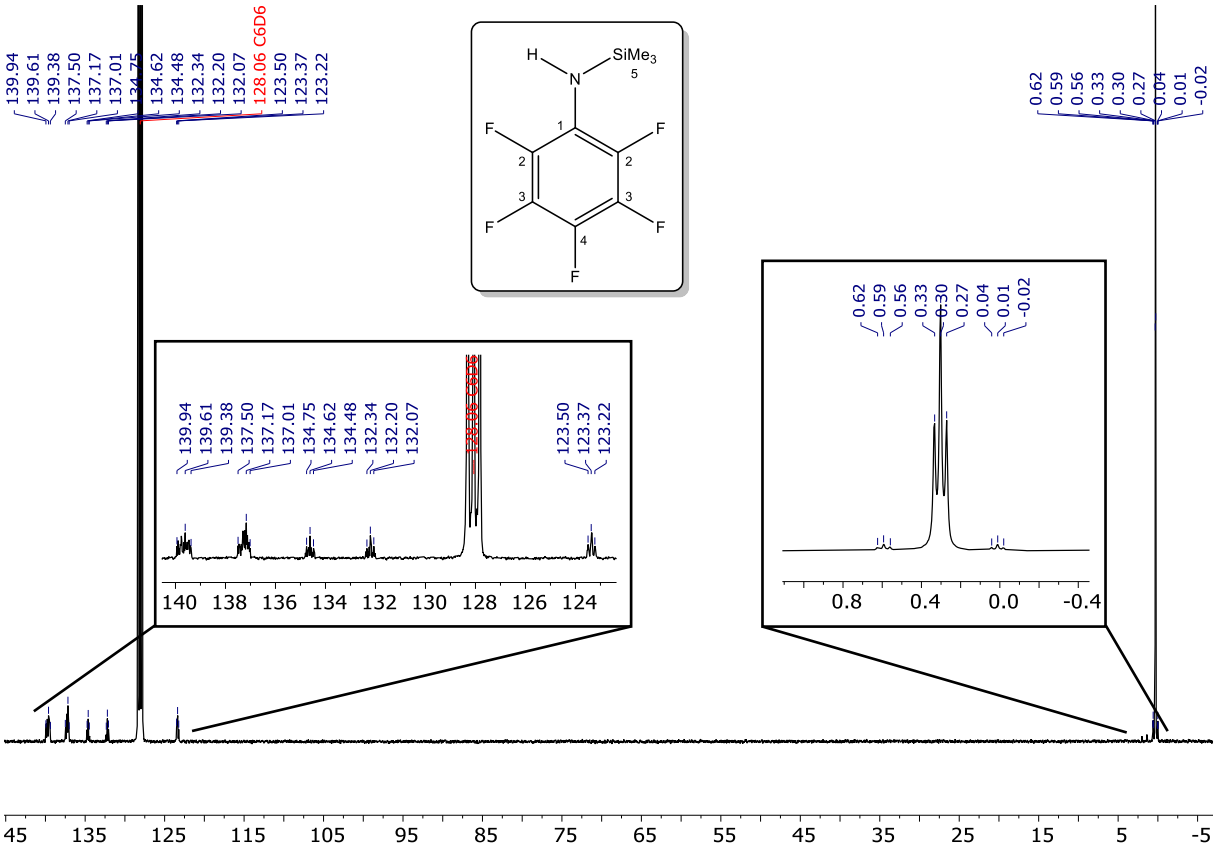

Fig. S15. $^{13}C\{^{1}H\}$ NMR spectrum (benzene-d_6, 100.62 MHz, 26 °C) of *N*-(pentafluorophenyl)-trimethylsilylamine (**3-H**).

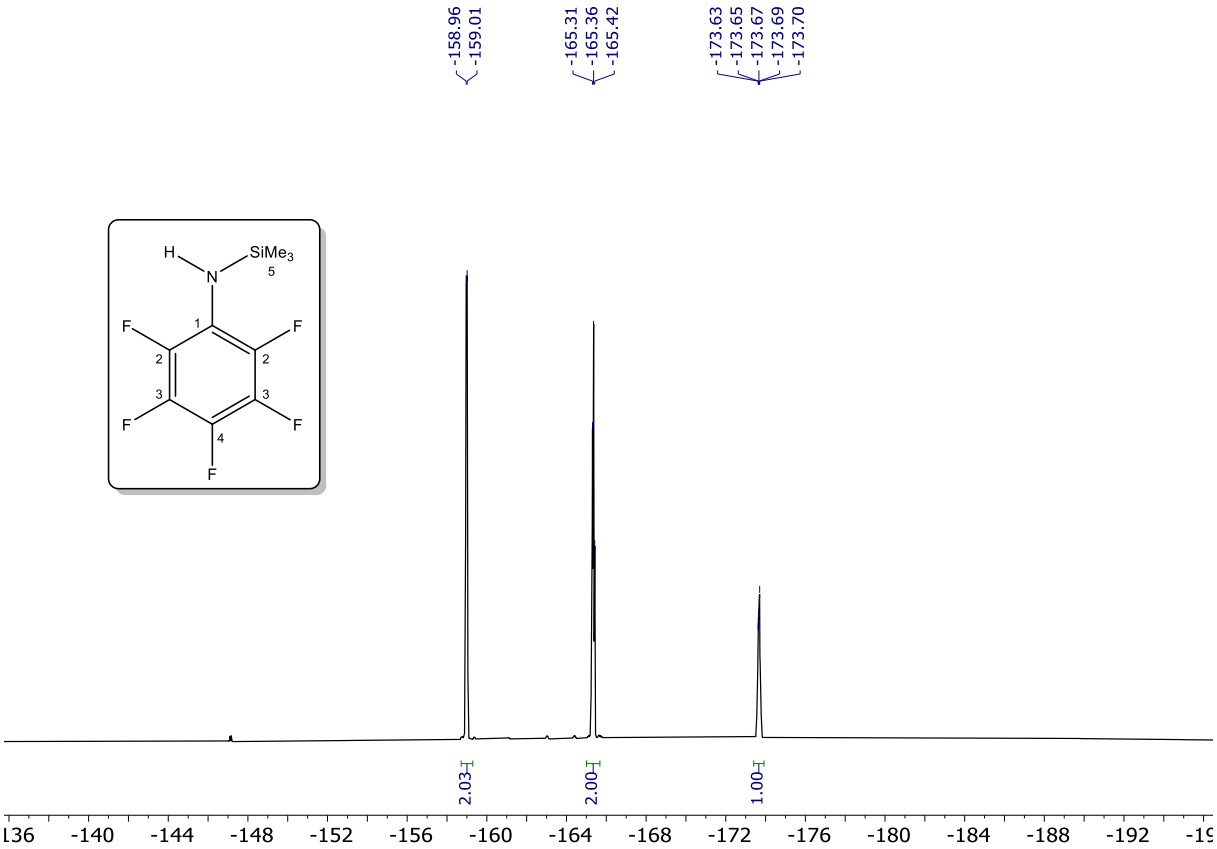

Fig. S16. ^{19}F NMR spectrum (benzene-d_6, 376.47 MHz, 25 °C) of *N*-(pentafluorophenyl)-trimethylsilylamine (**3-H**).

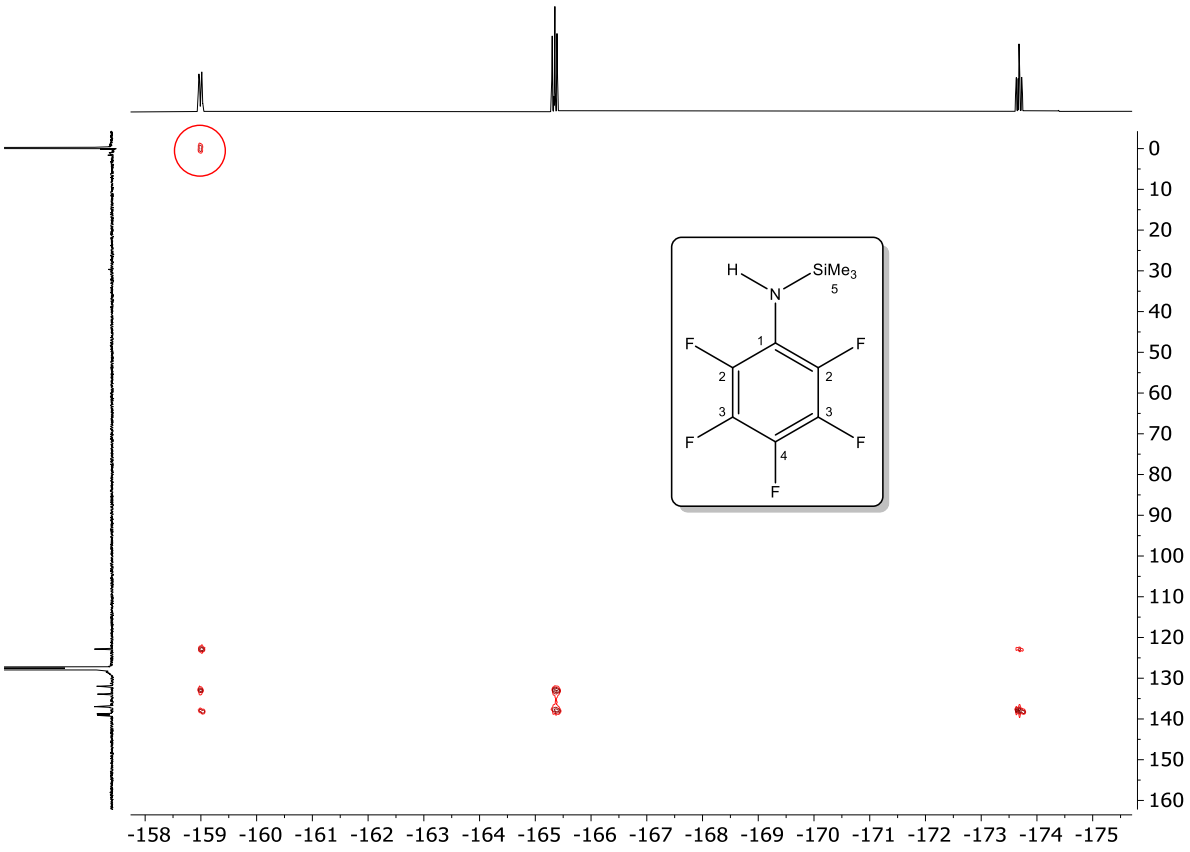

Fig. S17. HMBC ^{19}F-^{13}C NMR (benzene-d_6, 470.55/125.78 MHz, 27 °C) of *N*-(pentafluorophenyl)-trimethylsilylamine (**3-H**). The circled correlation spot demonstrates $^{5}J_{C,F}$ scalar coupling between *o-F* atoms and Si(CH_3) carbon atoms.

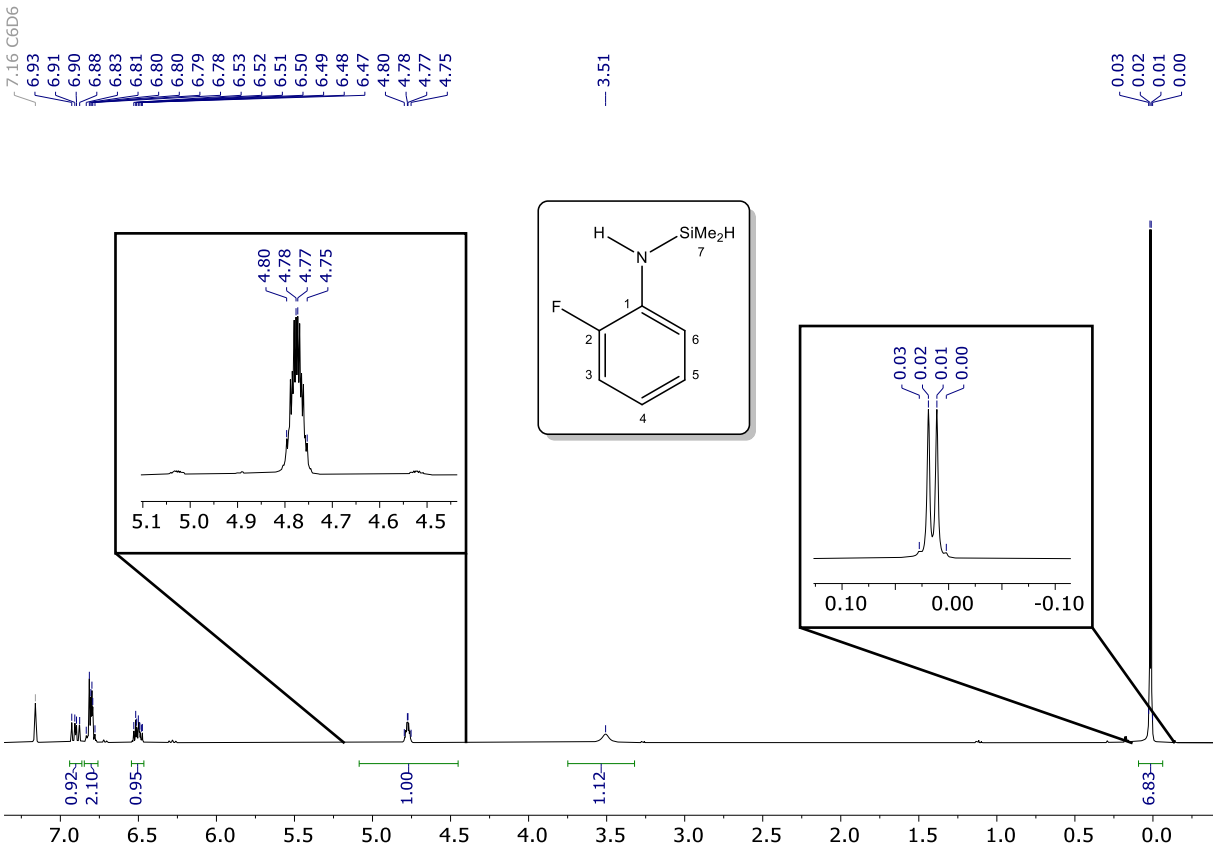

Fig. S18. ^{1}H NMR spectrum (benzene-d_6, 400.16 MHz, 27 °C) of *N*-(2-fluorophenyl)-dimethylsilylamine (**4-H**).

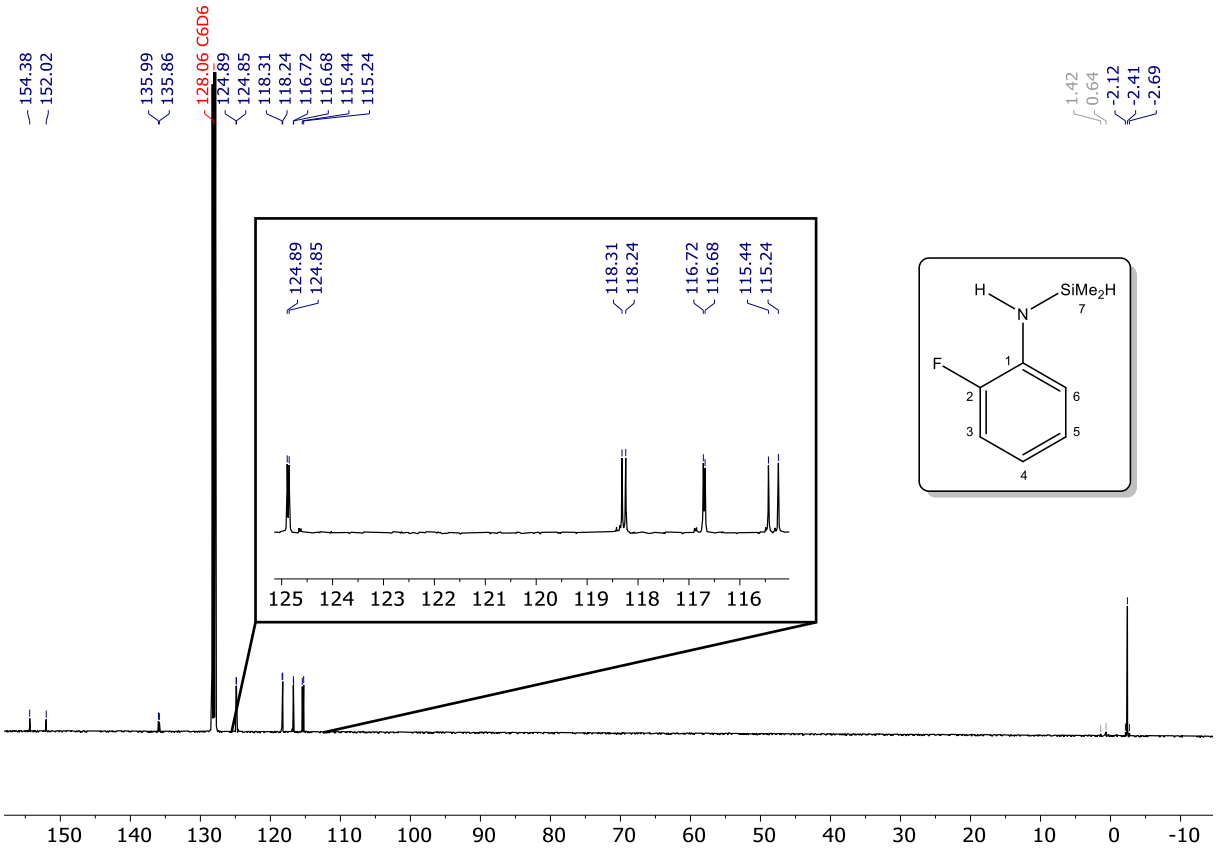

Fig. S19. $^{13}C\{^{1}H\}$ NMR spectrum (benzene-d_6, 100.62 MHz, 26 °C) of *N*-(2-fluorophenyl)-dimethylsilylamine (**4-H**).

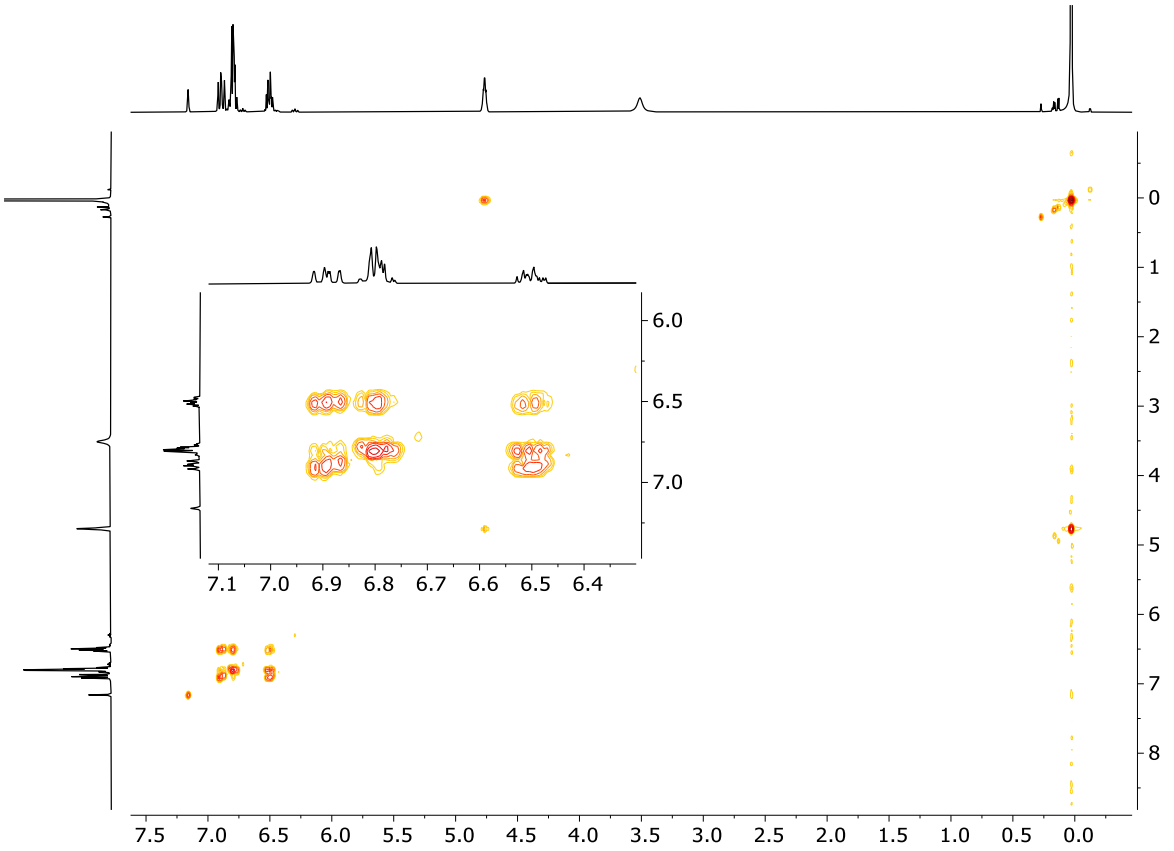

Fig. S20. COSY ^{1}H-^{1}H NMR (benzene-d_6, 400.16, 27 °C) of *N*-(2-fluorophenyl)-dimethylsilylamine (**4-H**).

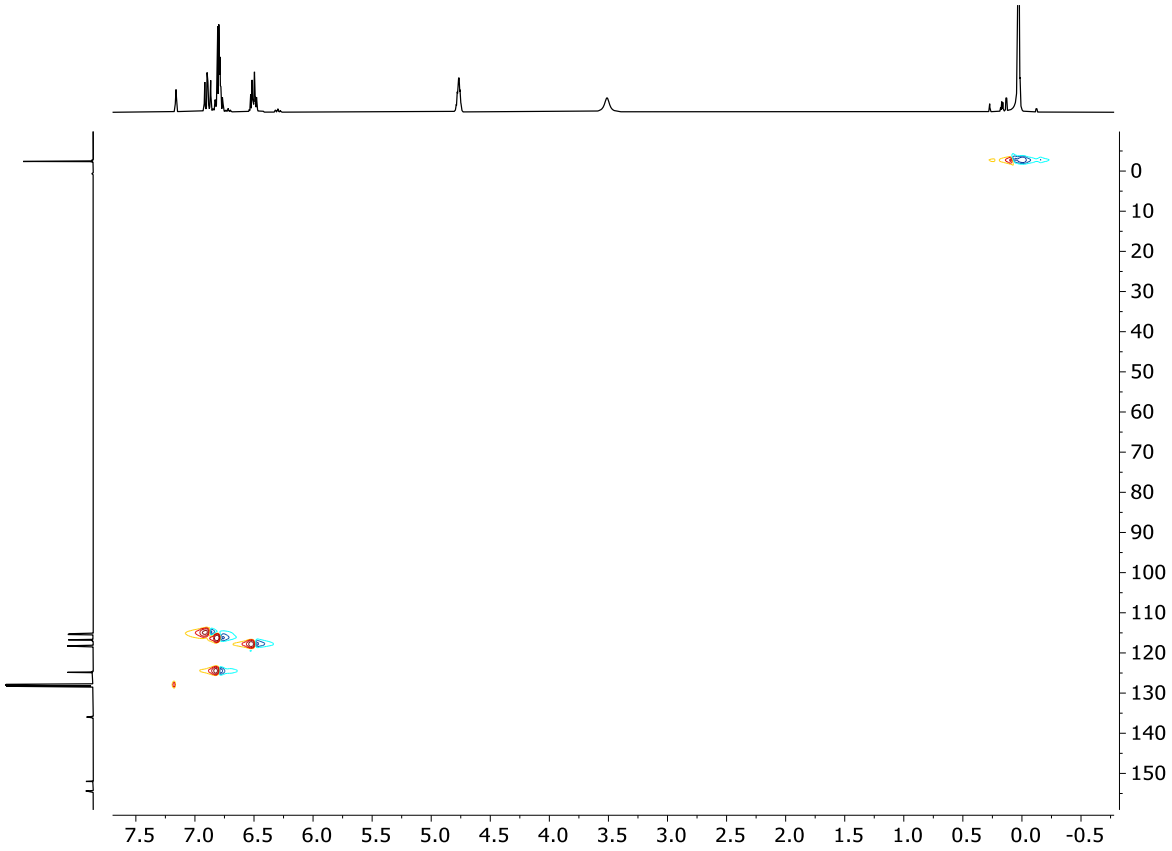

Fig. S21. HSQC ^{1}H-^{13}C NMR (benzene-d_6, 400.16/100.63 MHz, 27 °C) of *N*-(2-fluorophenyl)-dimethylsilylamine (**4-H**).

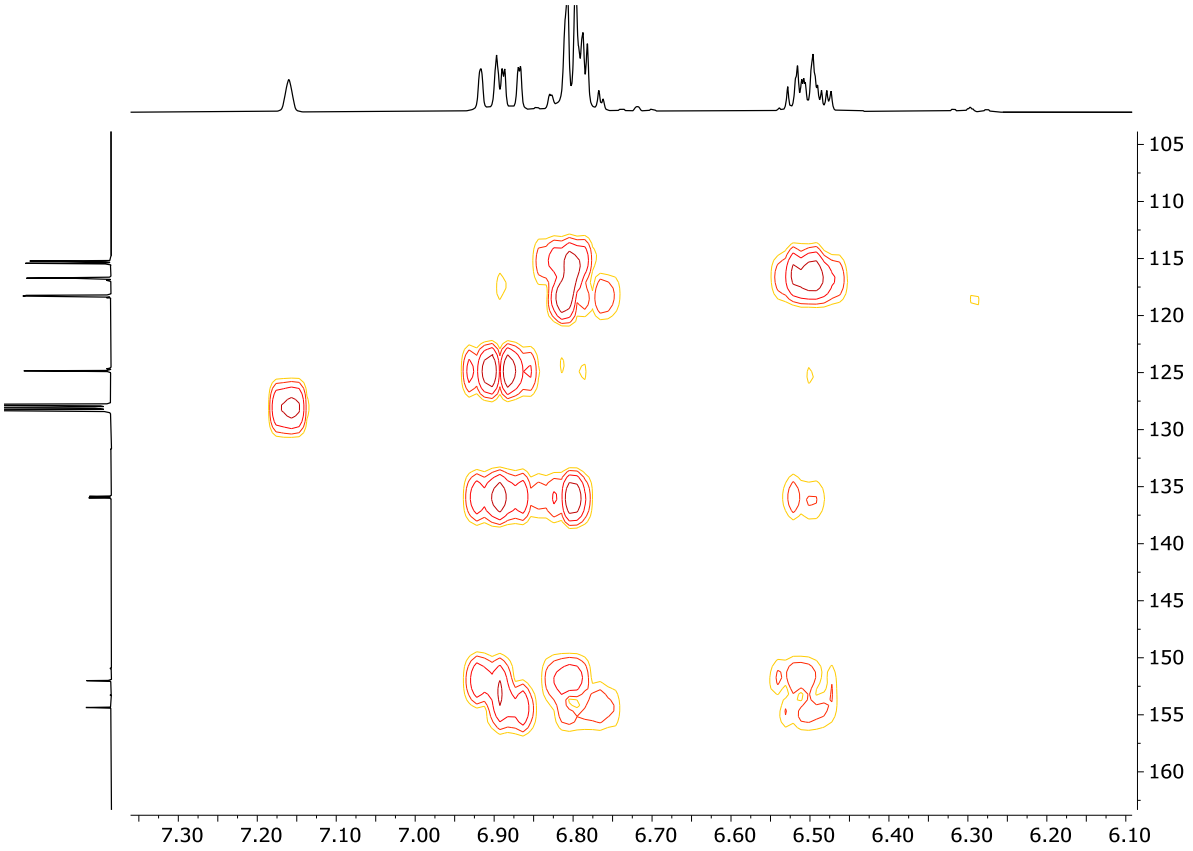

Fig. S22. HMBC ^{1}H-^{13}C NMR (benzene-d_6, 400.16/100.63 MHz, 27 °C) of *N*-(2-fluorophenyl)-dimethylsilylamine (**4-H**).

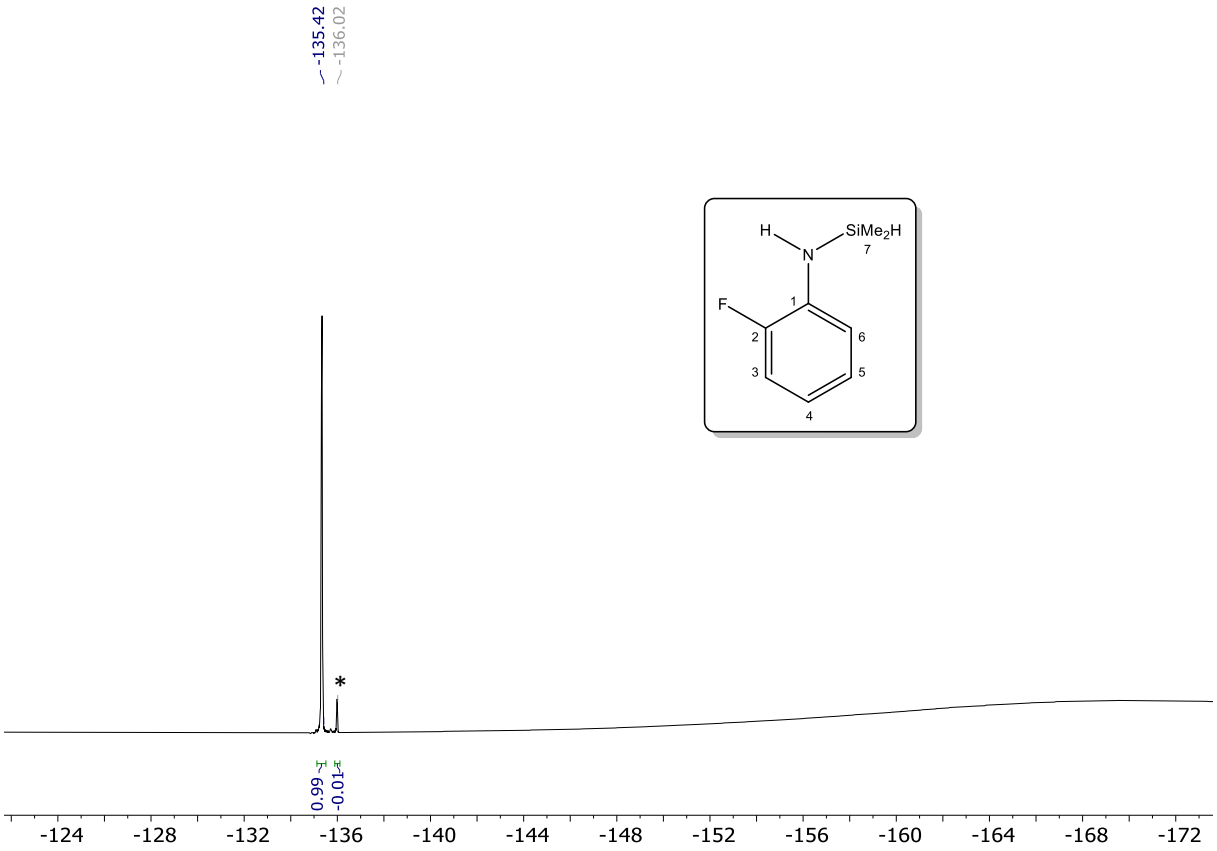

Fig. S23. ^{19}F NMR spectrum (benzene-d_6, 376.44 MHz, 24 °C) of *N*-(2-fluorophenyl)-dimethylsilylamine (**4-H**). * = impurity (ca. 1 mol-%).

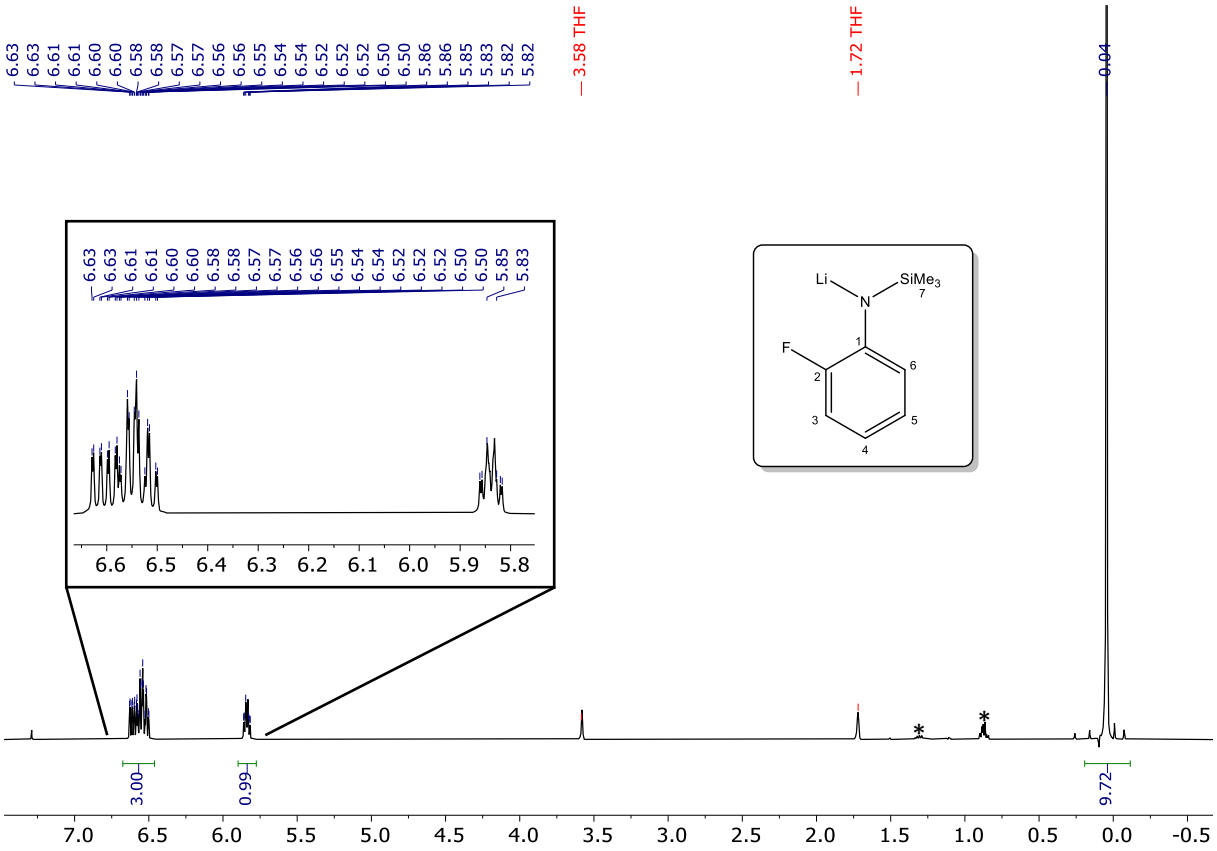

Fig. S24. ^{1}H NMR spectrum (thf-d_8, 500.13 MHz, 27 °C) of *N*-(2-fluorophenyl)-trimethylsilylamide (**1-Li**). * = residual solvent (petroleum ether).

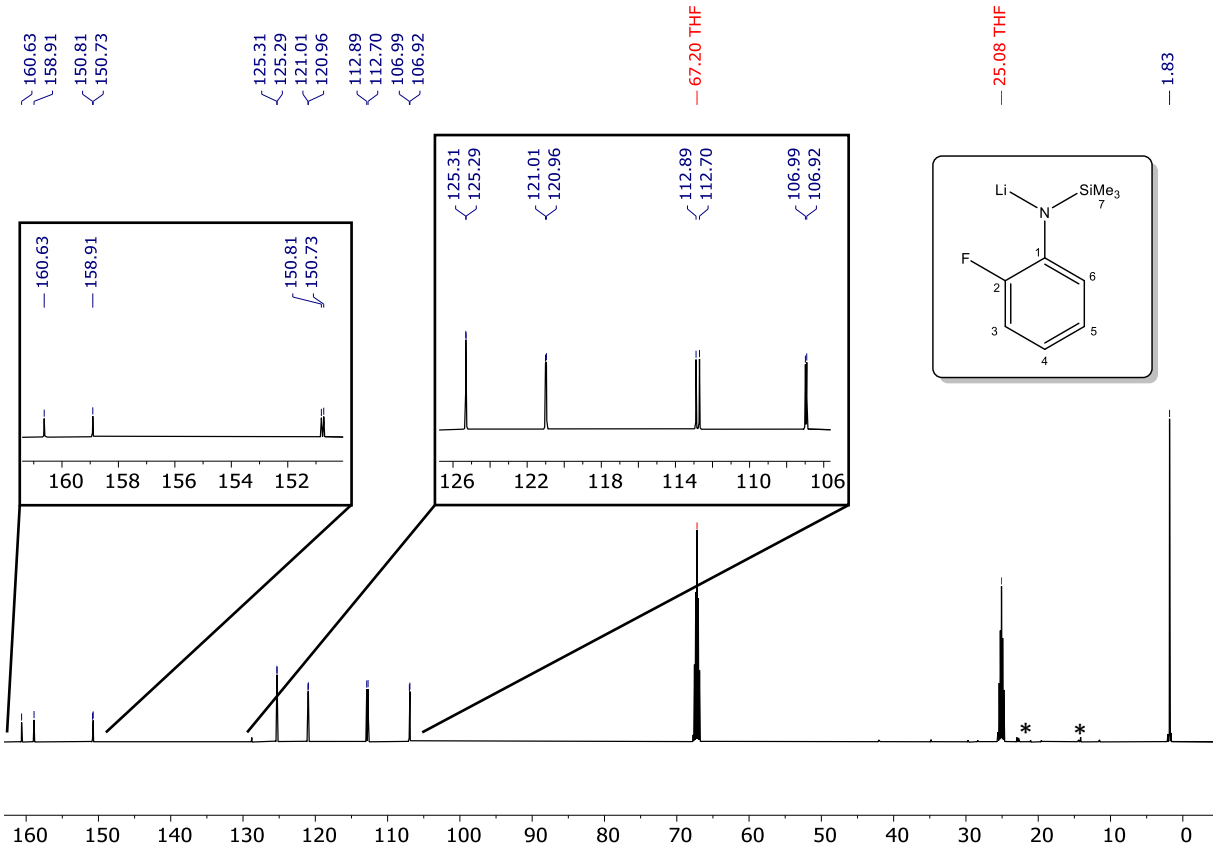

Fig. S25. $^{13}C\{^{1}H\}$ NMR spectrum (thf-d_8, 125.77 MHz, 27 °C) of *N*-(2-fluorophenyl)-trimethylsilylamide (**1-Li**). * = residual solvent (petroleum ether).

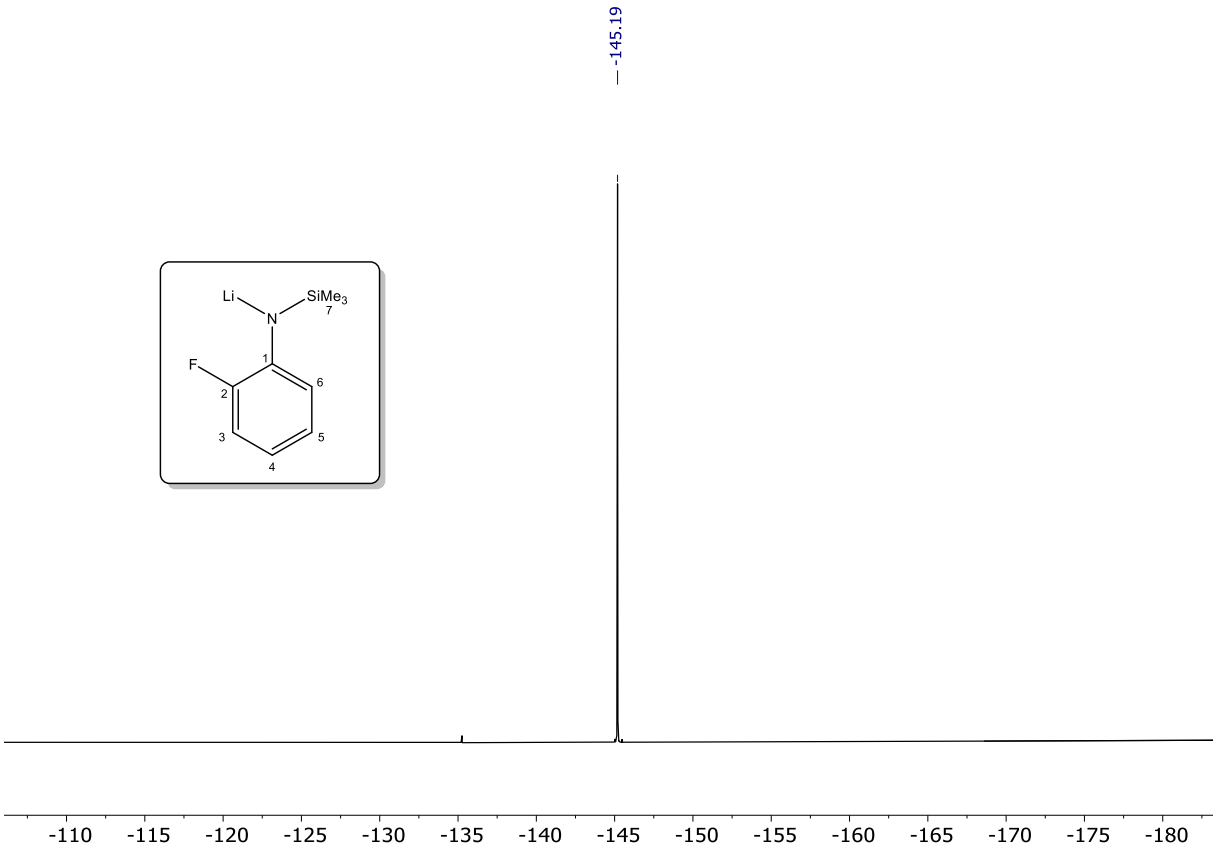

Fig. S26. ^{19}F NMR spectrum (thf-d_8, 470.52 MHz, 27 °C) of *N*-(2-fluorophenyl)-trimethylsilylamide (**1-Li**).

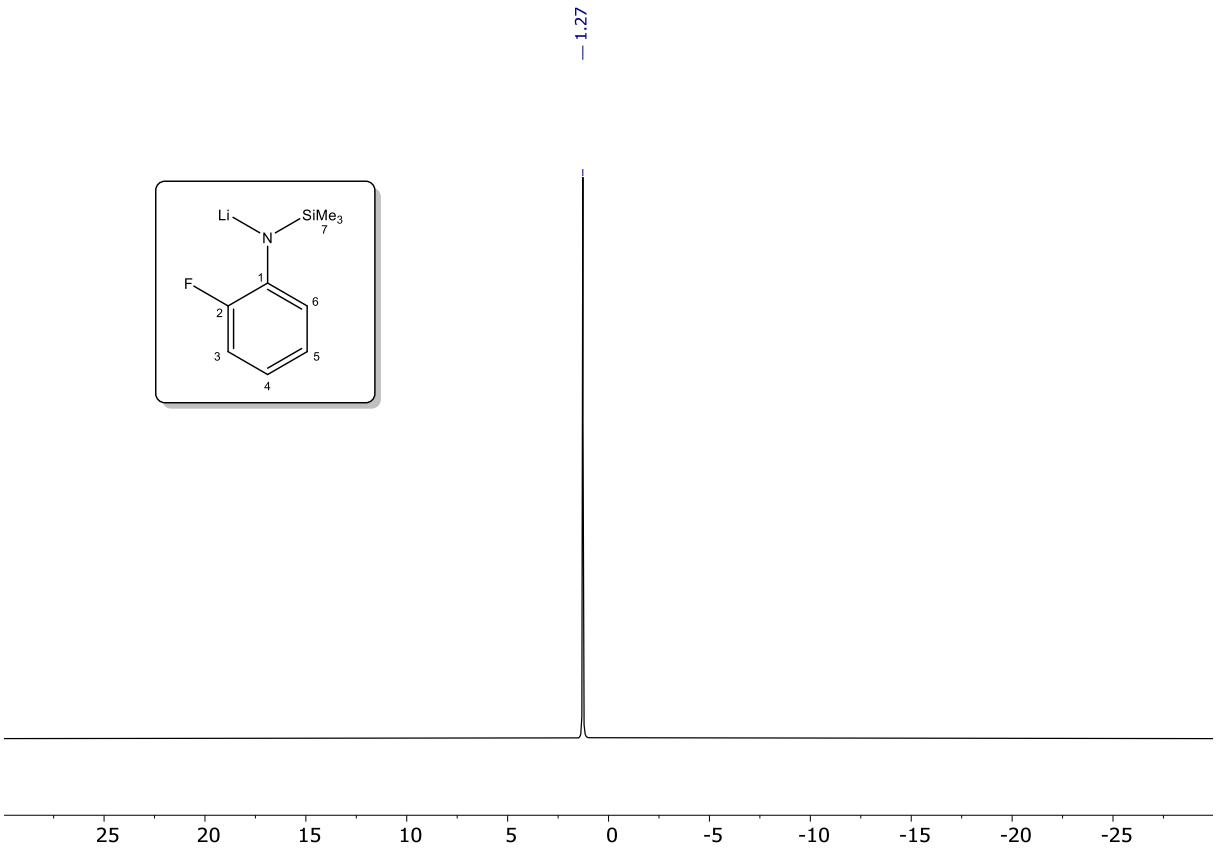

Fig. S27. ^{7}Li NMR spectrum (thf-d_8, 194.37 MHz, 27 °C) of *N*-(2-fluorophenyl)-trimethylsilylamide (**1-Li**).

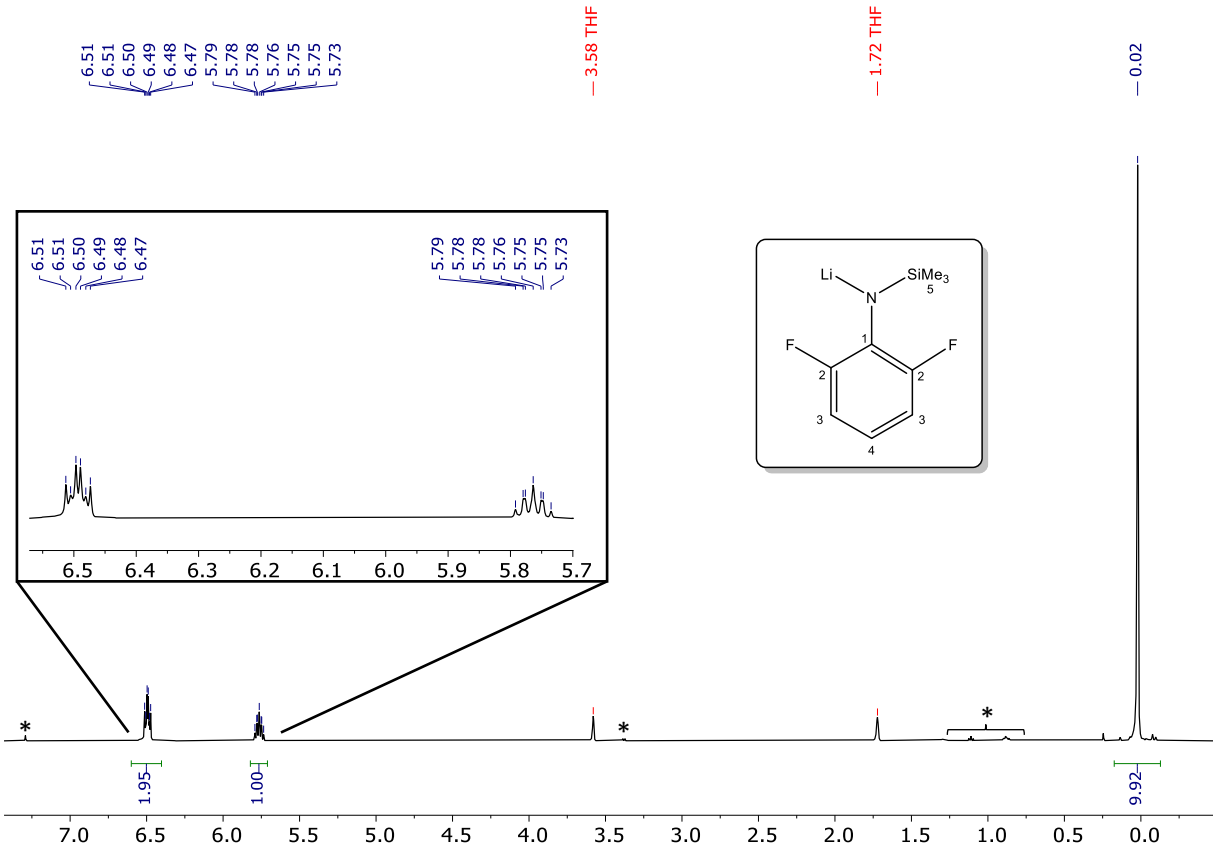

Fig. S28. ^{1}H NMR spectrum (thf-d_8, 500.13 MHz, 27 °C) of *N*-(2,6-difluorophenyl)-trimethylsilylamide (**2-Li**). * = residual solvent (benzene, petroleum ether and Et_2O).

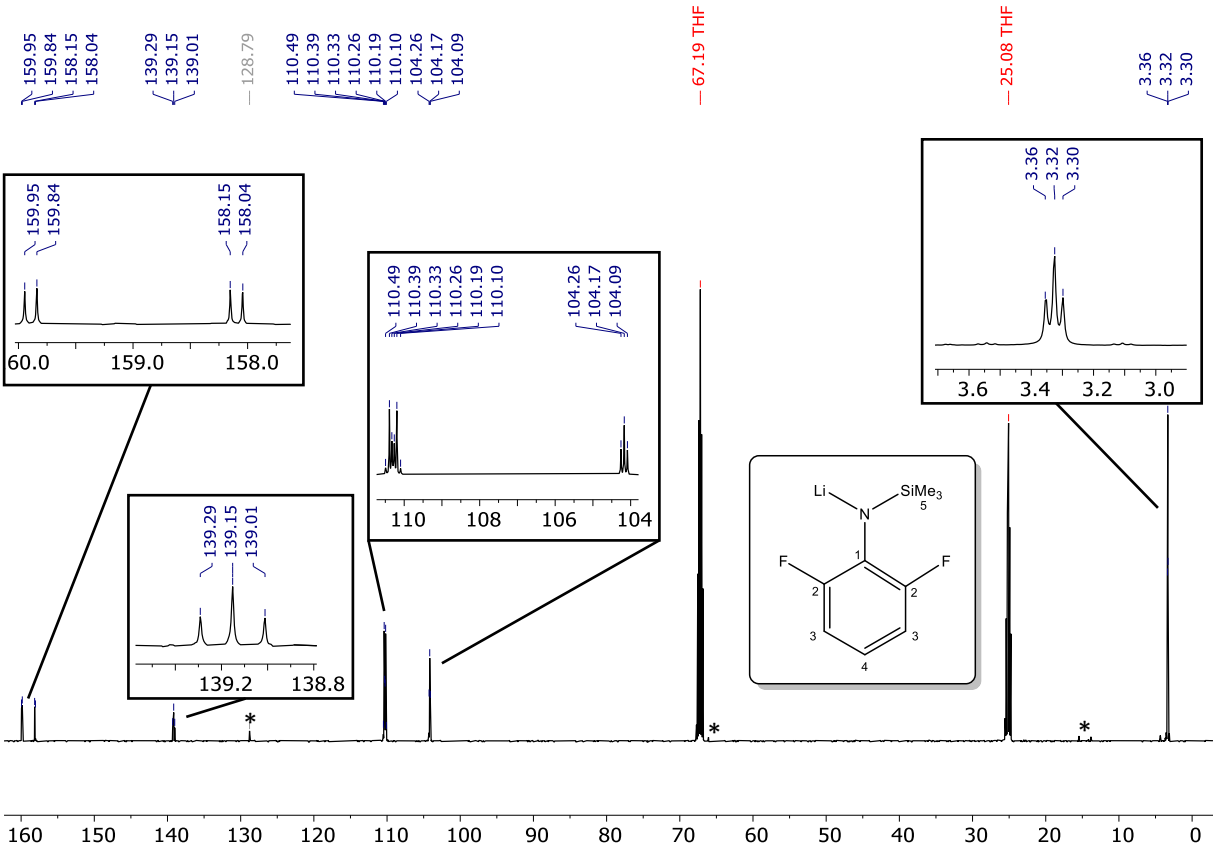

Fig. S29. $^{13}C\{^{1}H\}$ NMR spectrum (thf-d_8, 125.77 MHz, 27 °C) of *N*-(2,6-difluorophenyl)-trimethylsilylamide (**2-Li**). * = residual solvent (petroleum ether, Et_2O and benzene).

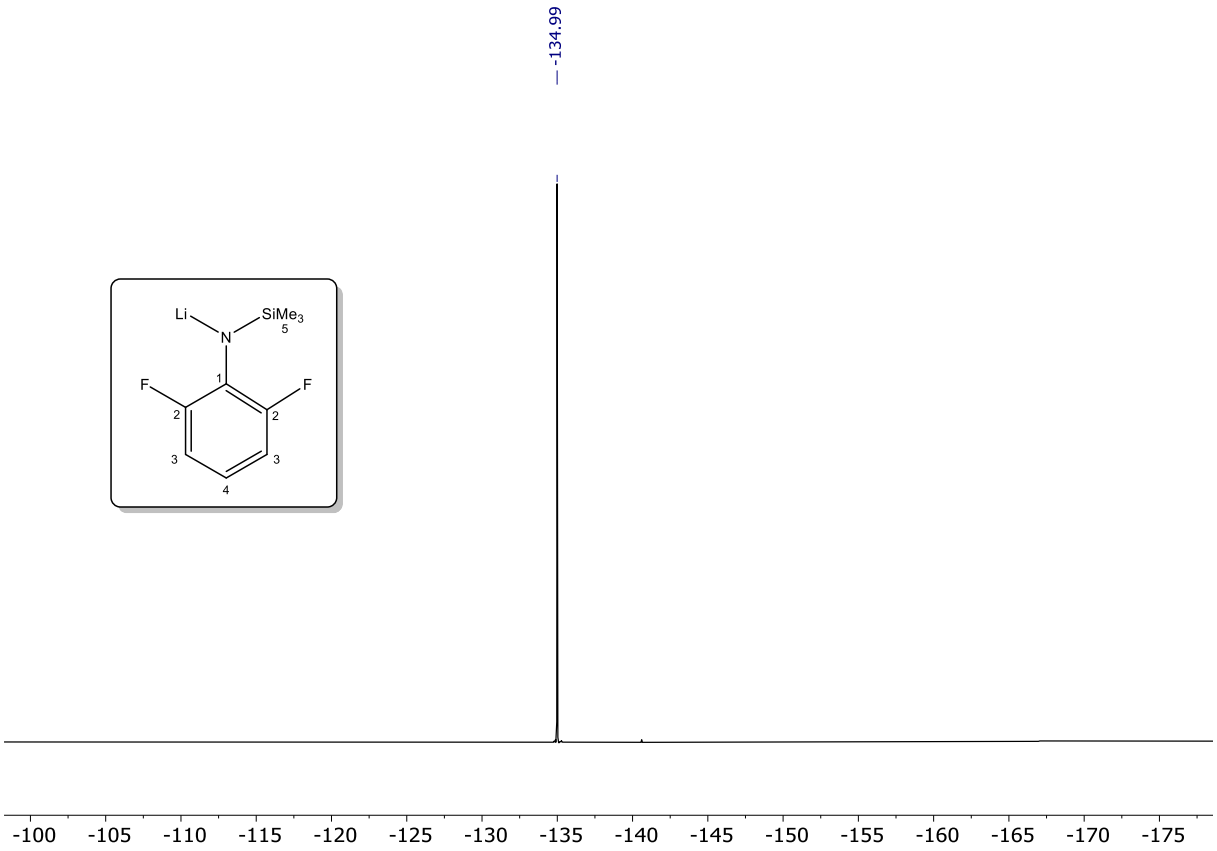

Fig. S30. ^{19}F NMR spectrum (thf-d_8, 470.52 MHz, 27 °C) of *N*-(2,6-difluorophenyl)-trimethylsilylamide (**2-Li**).

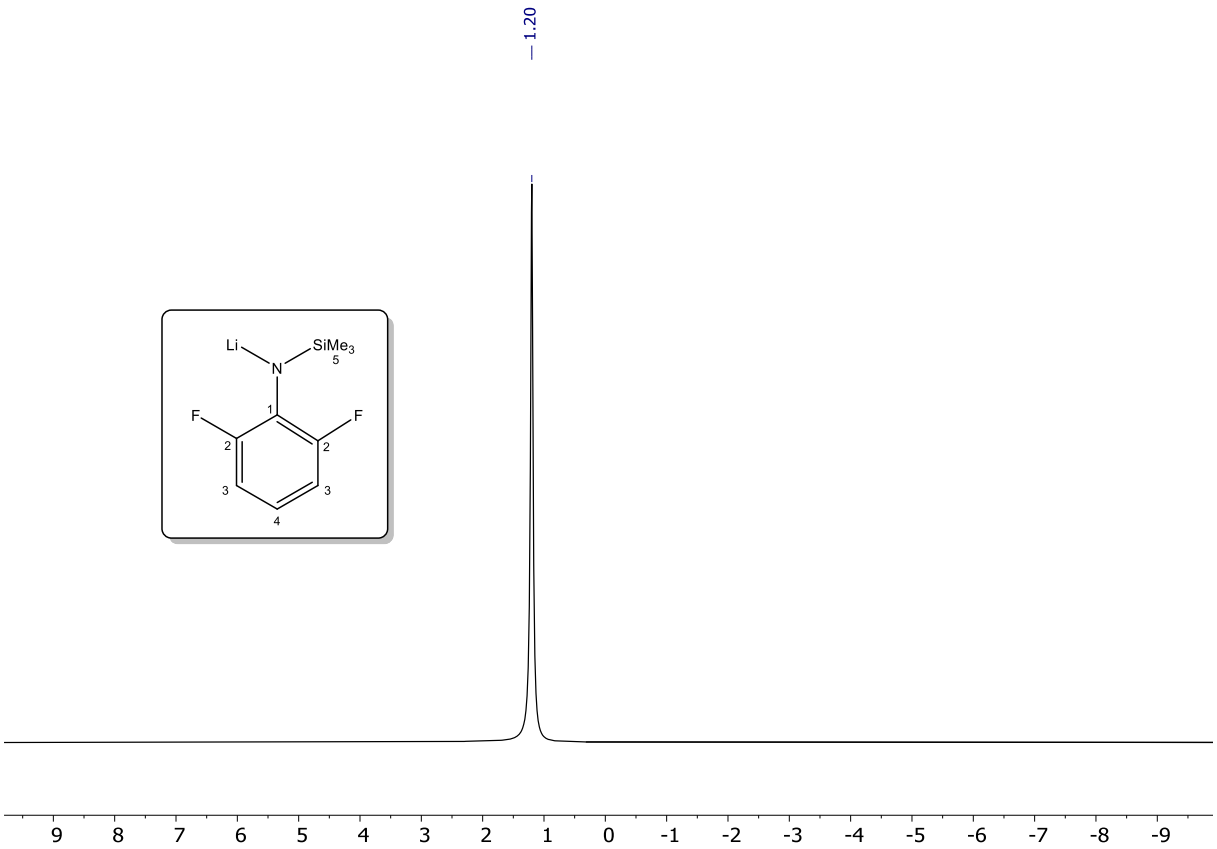

Fig. S31. ^{7}Li NMR spectrum (thf-d_8, 194.37 MHz, 27 °C) of *N*-(2,6-difluorophenyl)-trimethylsilylamide (**2-Li**).

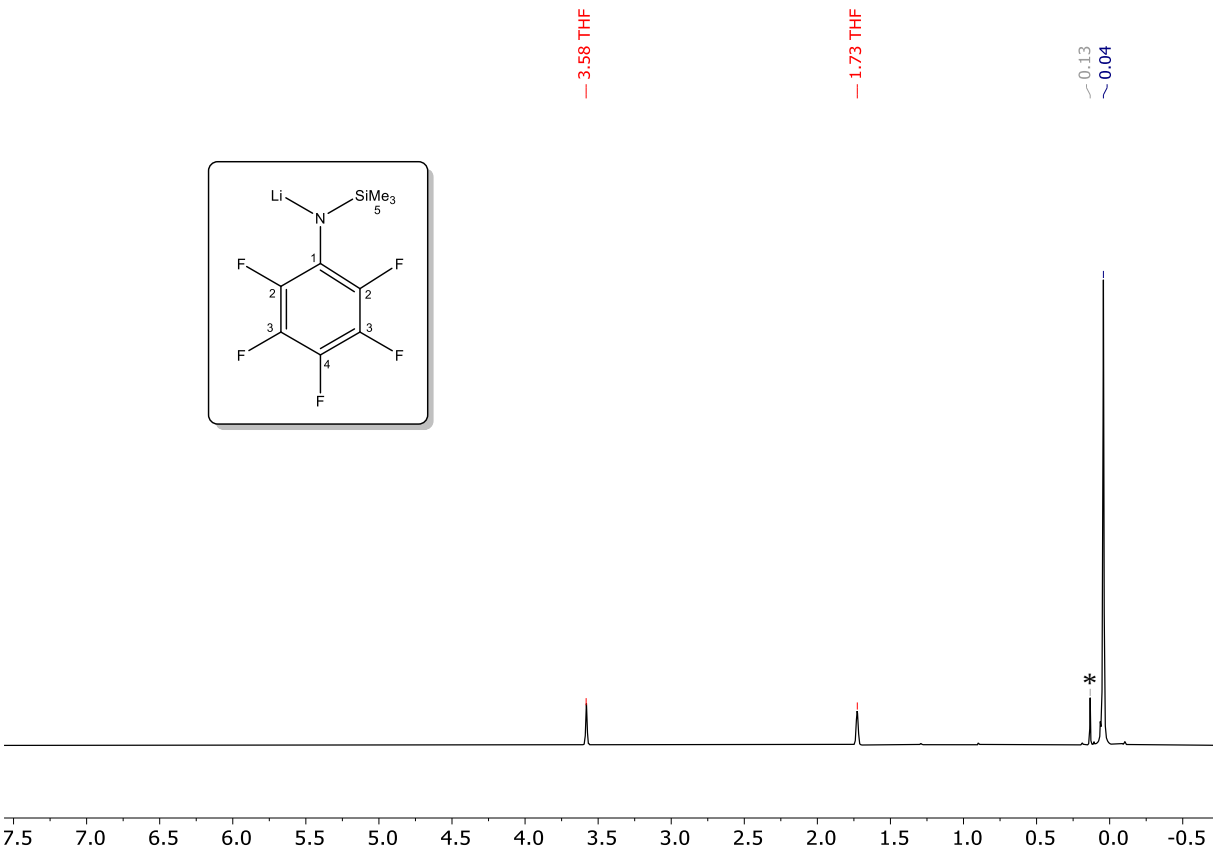

Fig. S32. ^{1}H NMR spectrum (thf-d_8, 500.13 MHz, 27 °C) of *N*-(pentafluorophenyl)-trimethylsilylamide (**3-Li**). * = hydrolysed complex.

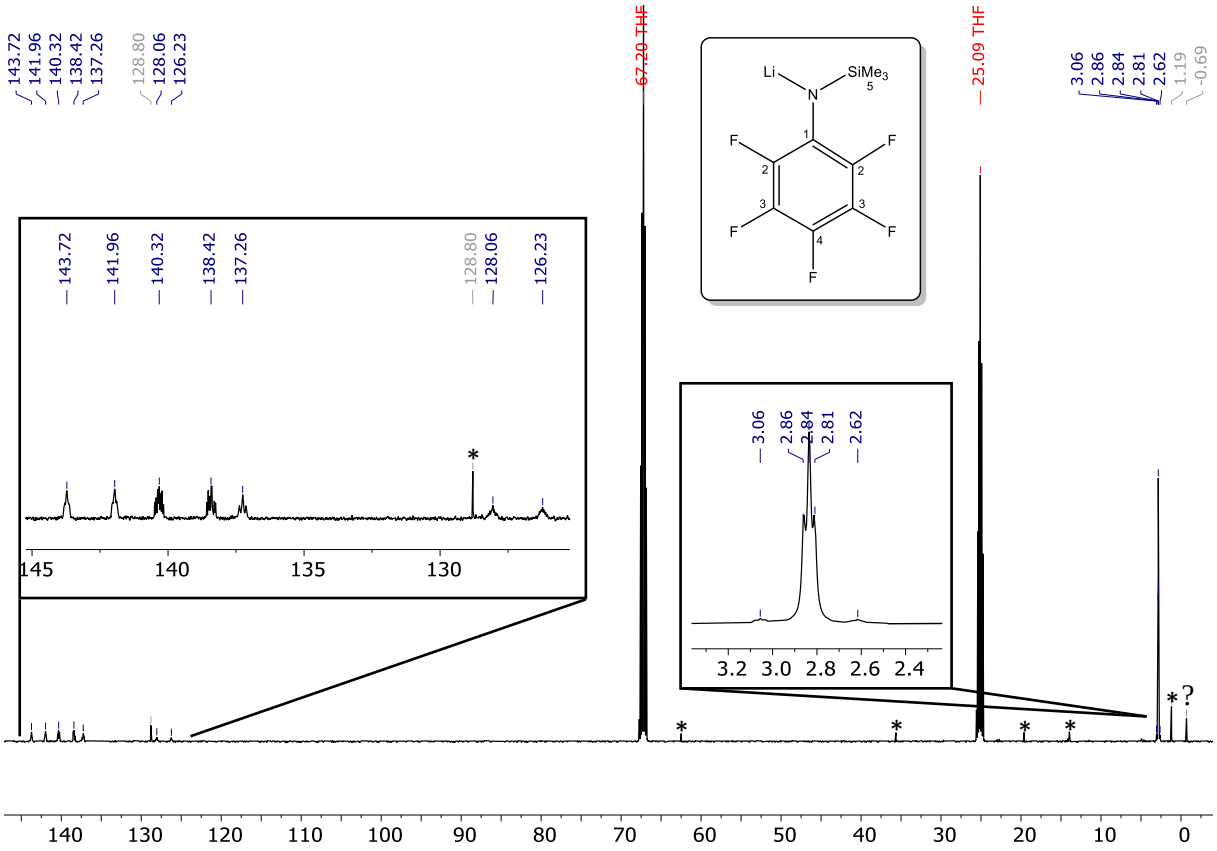

Fig. S33. $^{13}C\{^{1}H\}$ NMR spectrum (thf-d_8, 125.77 MHz, 27 °C) of *N*-(pentafluorophenyl)-trimethylsilylamide (**3-Li**). * = residual solvent (silicone grease, benzene and petroleum ether). ? = unknown decomposition product (most probably hydrolysed complex).

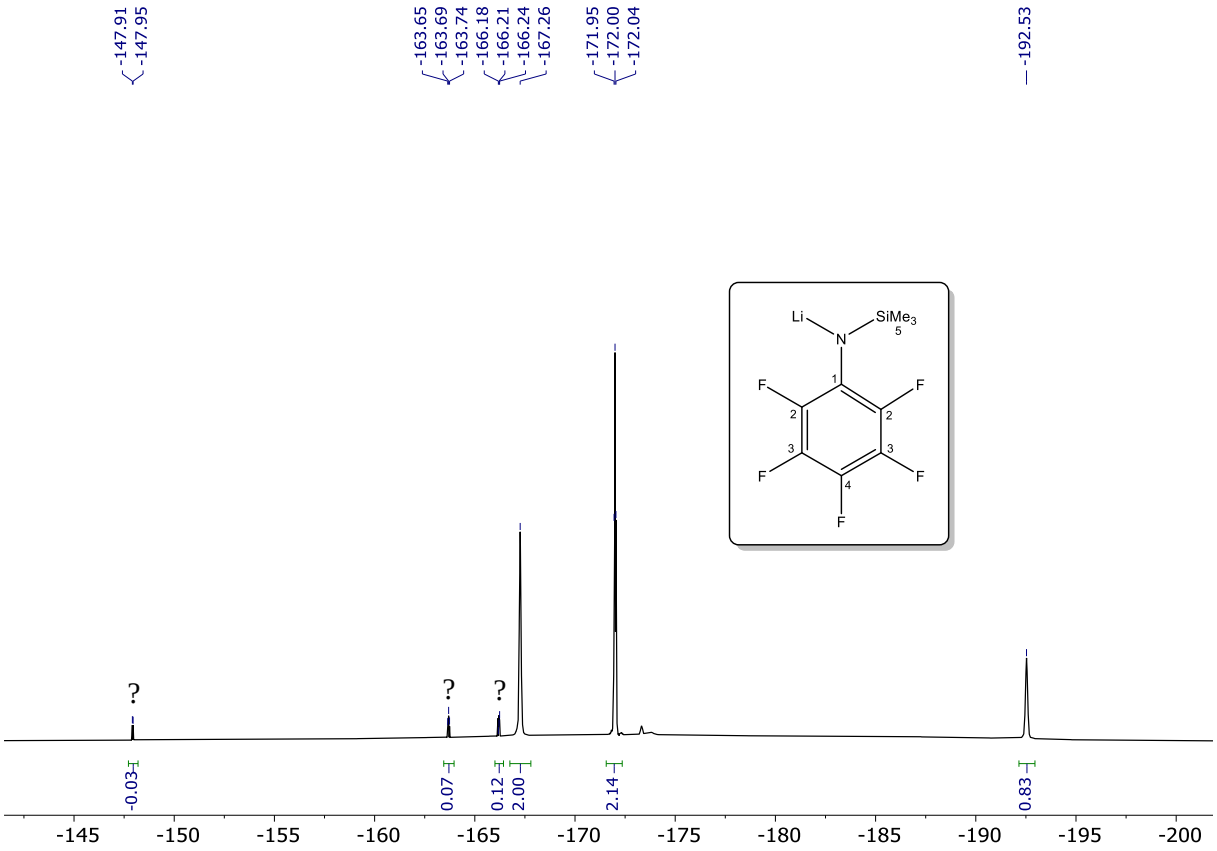

Fig. S34. ^{19}F NMR spectrum (thf-d_8, 470.52 MHz, 27 °C) of *N*-(pentafluorophenyl)-trimethylsilylamide (**3-Li**). ? = unidentified side or decomposition product, ca. 4 mol-%.

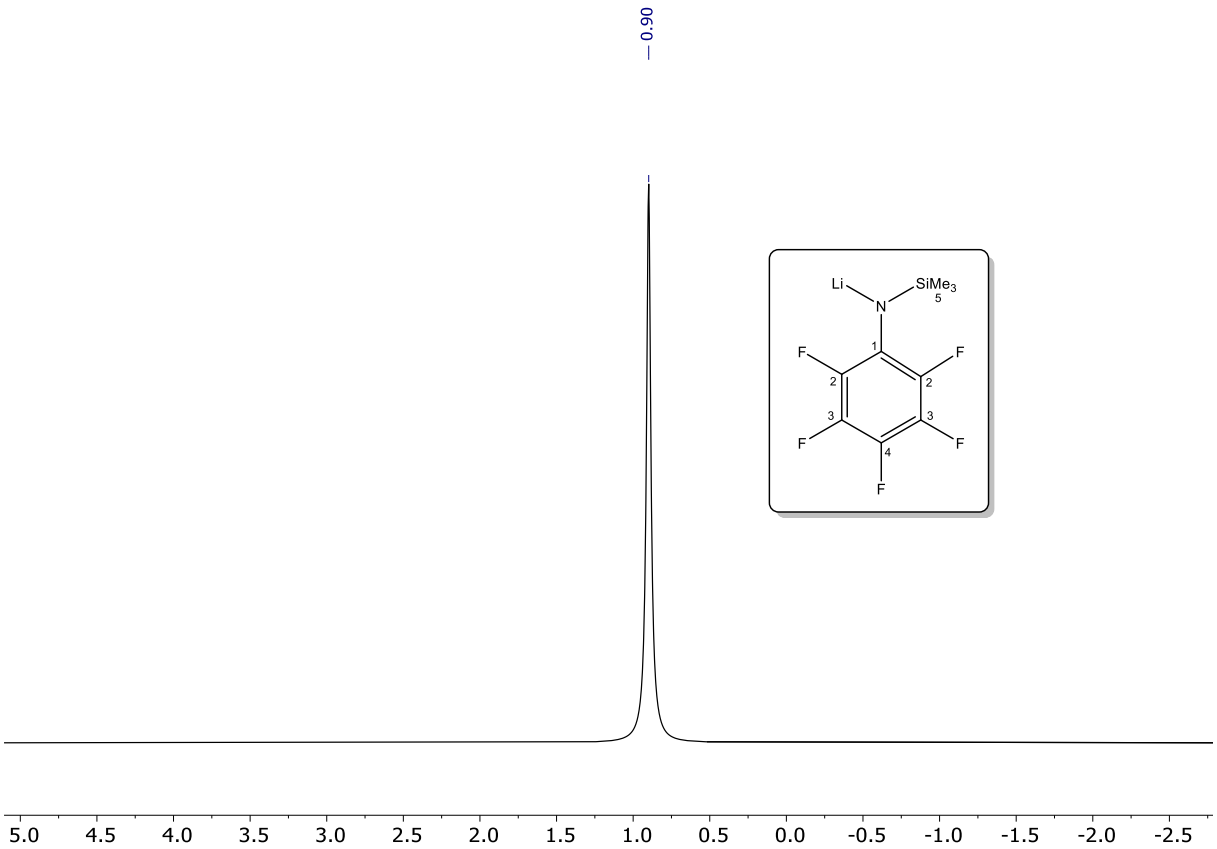

Fig. S35. ^{7}Li NMR spectrum (thf-d_8, 155.51 MHz, 25 °C) of *N*-(pentafluorophenyl)-trimethylsilylamide (**3-Li**).

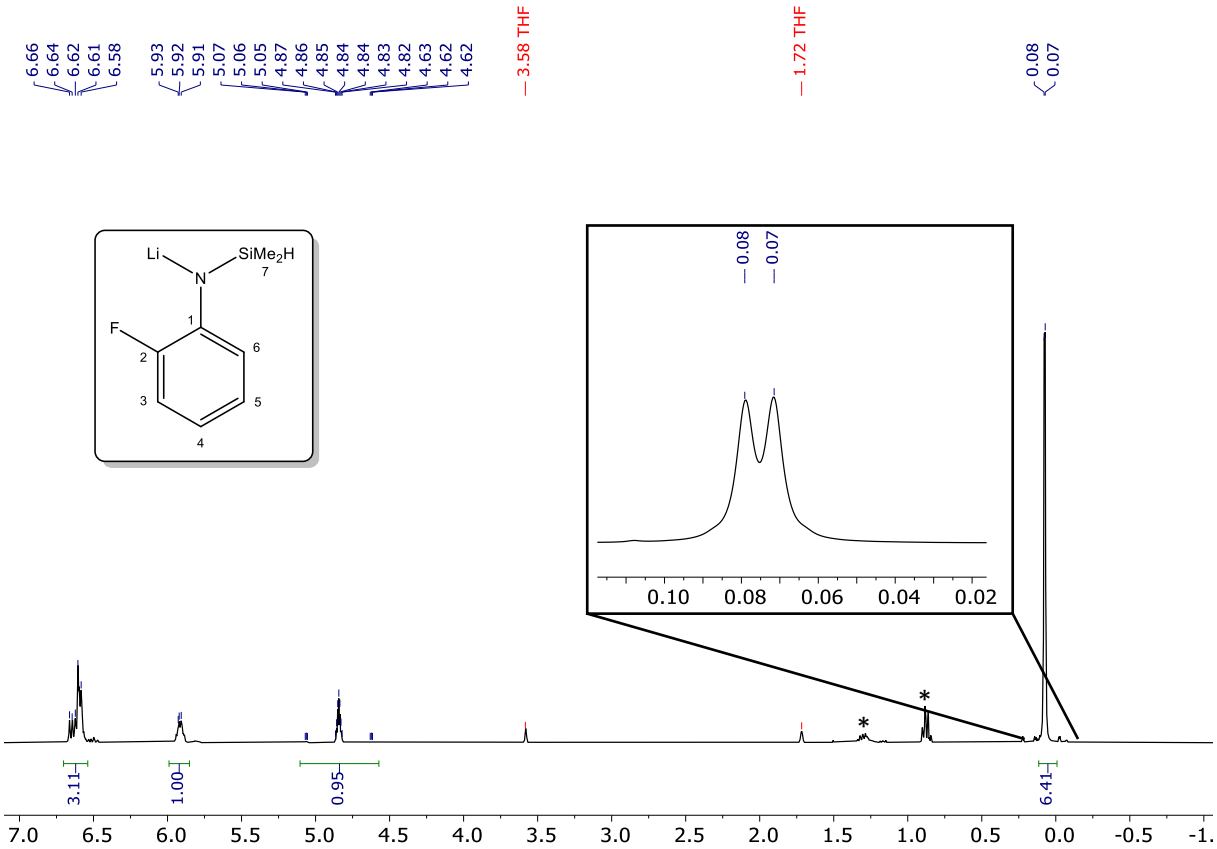

Fig. S36. ^{1}H NMR spectrum (thf-d_8, 400.13 MHz, 25 °C) of *N*-(2-fluorophenyl)-dimethylsilylamide (**4-Li**). * = residual petroleum ether.

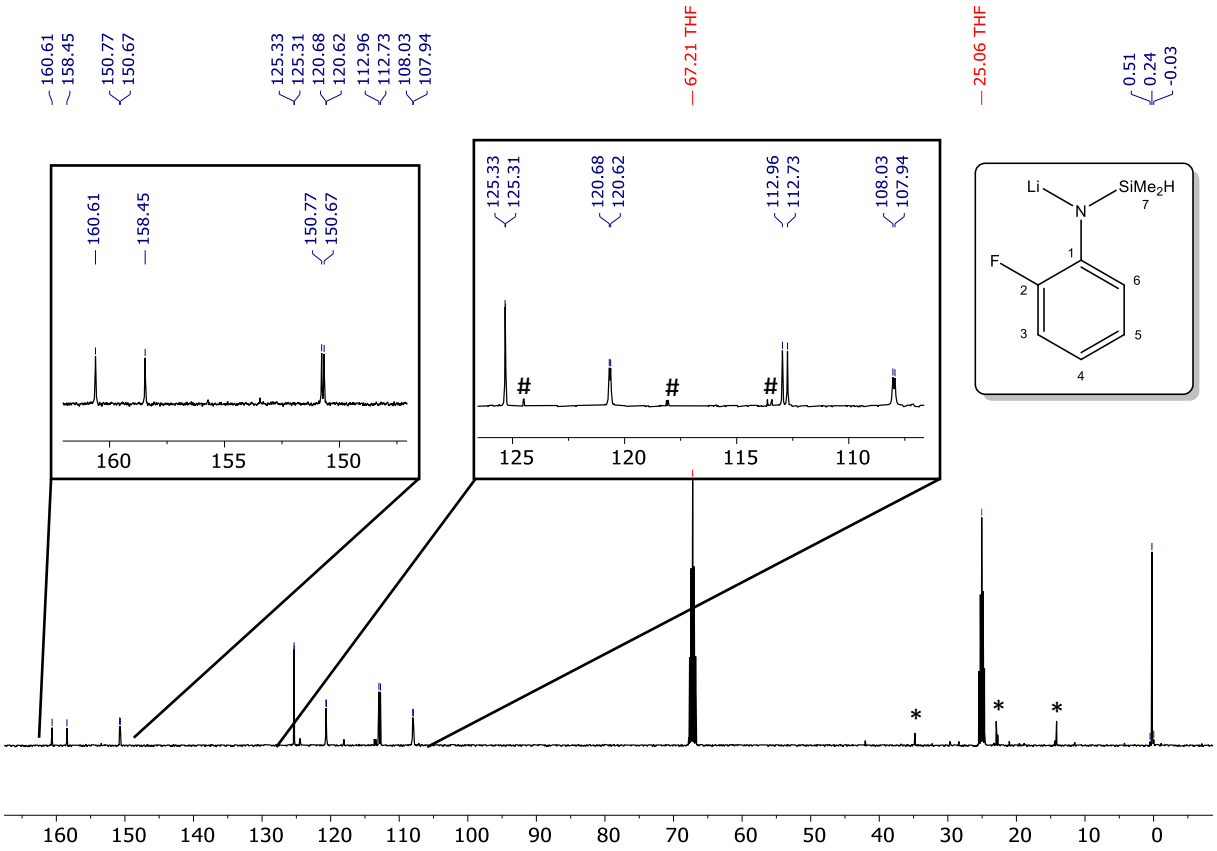

Fig. S37. $^{13}C\{^{1}H\}$ NMR spectrum (thf-d_8, 100.62, 26 °C) of *N*-(2-fluorophenyl)-dimethylsilylamide (**4-Li**). * = residual petroleum ether. Some partial hydrolysis (#) was observed after several hours.

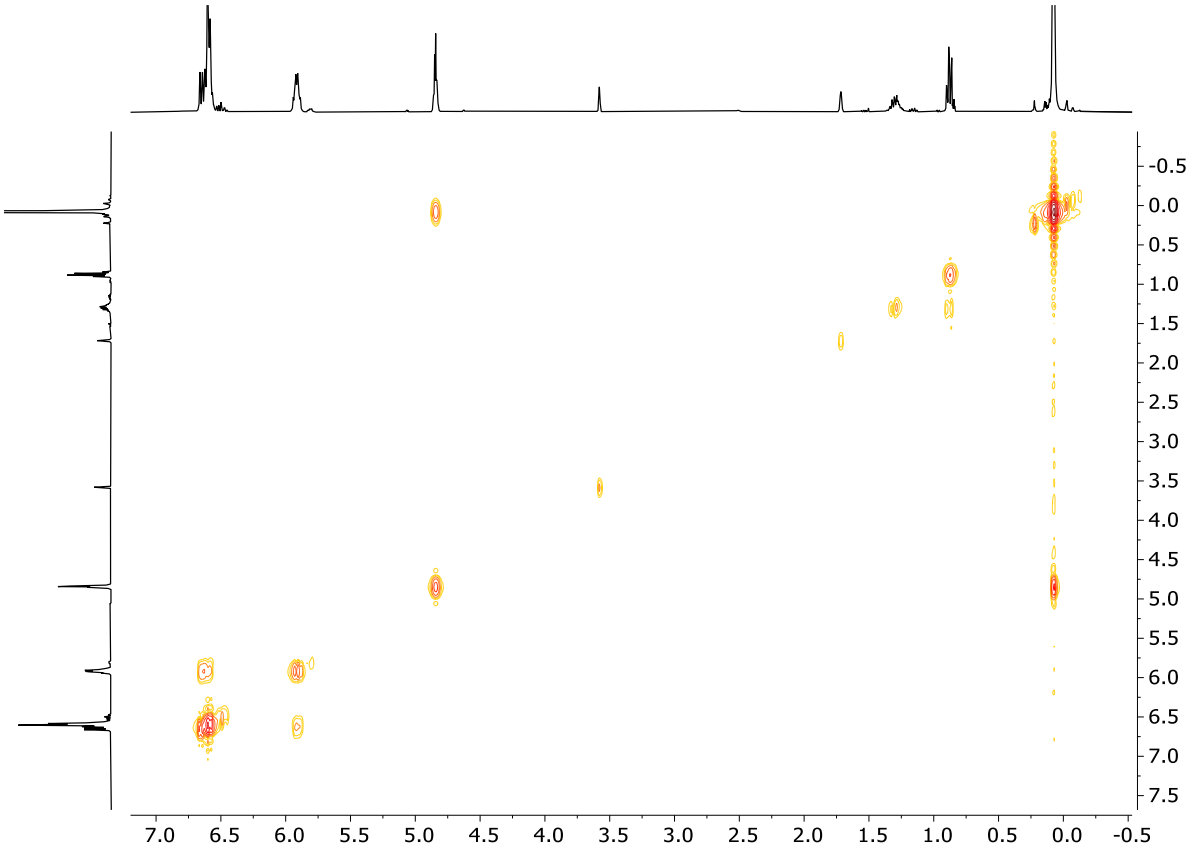

Fig. S38. COSY ^{1}H-^{1}H NMR (benzene-d_6, 400.16 MHz, 27 °C) of *N*-(2-fluorophenyl)-dimethylsilylamide (**4-Li**).

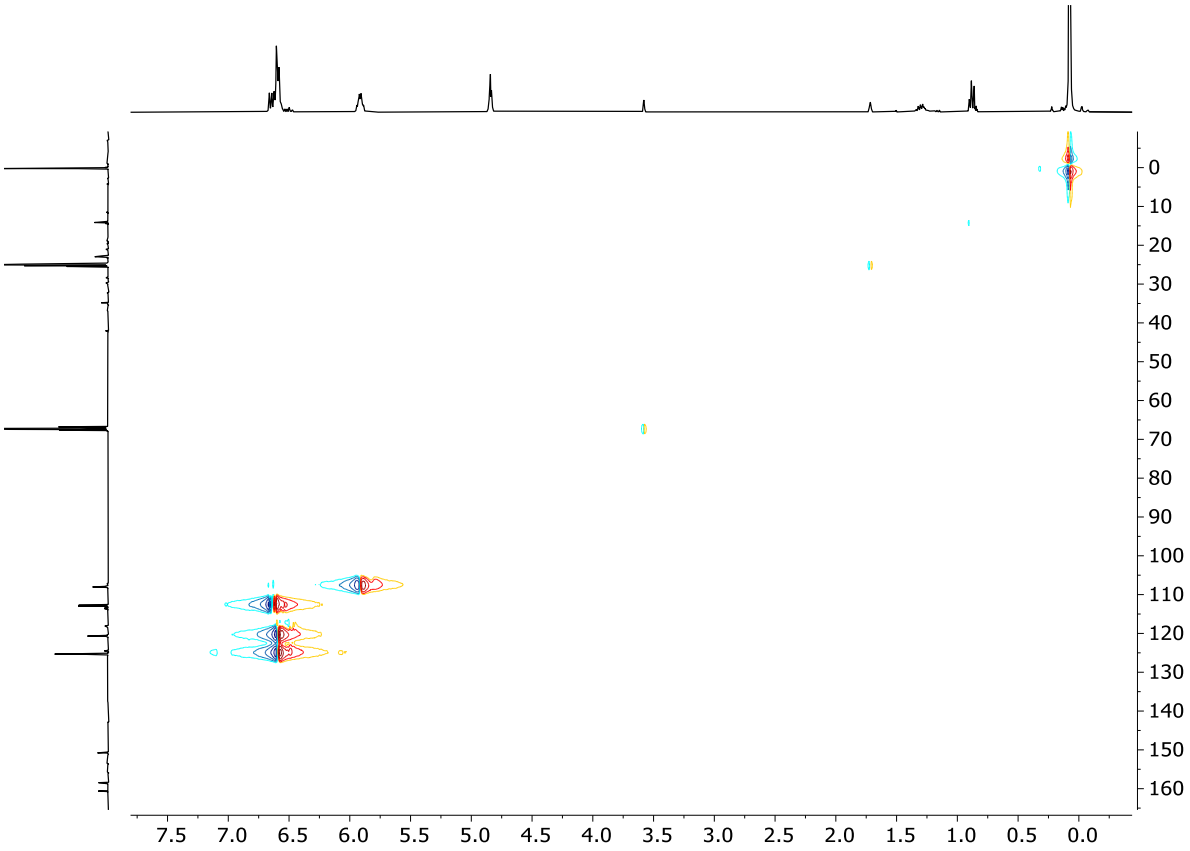

Fig. S39. HSQC ^{1}H-^{13}C NMR (benzene-d_6, 400.16/100.63 MHz, 27 °C) of *N*-(2-fluorophenyl)-dimethylsilylamide (**4-Li**).

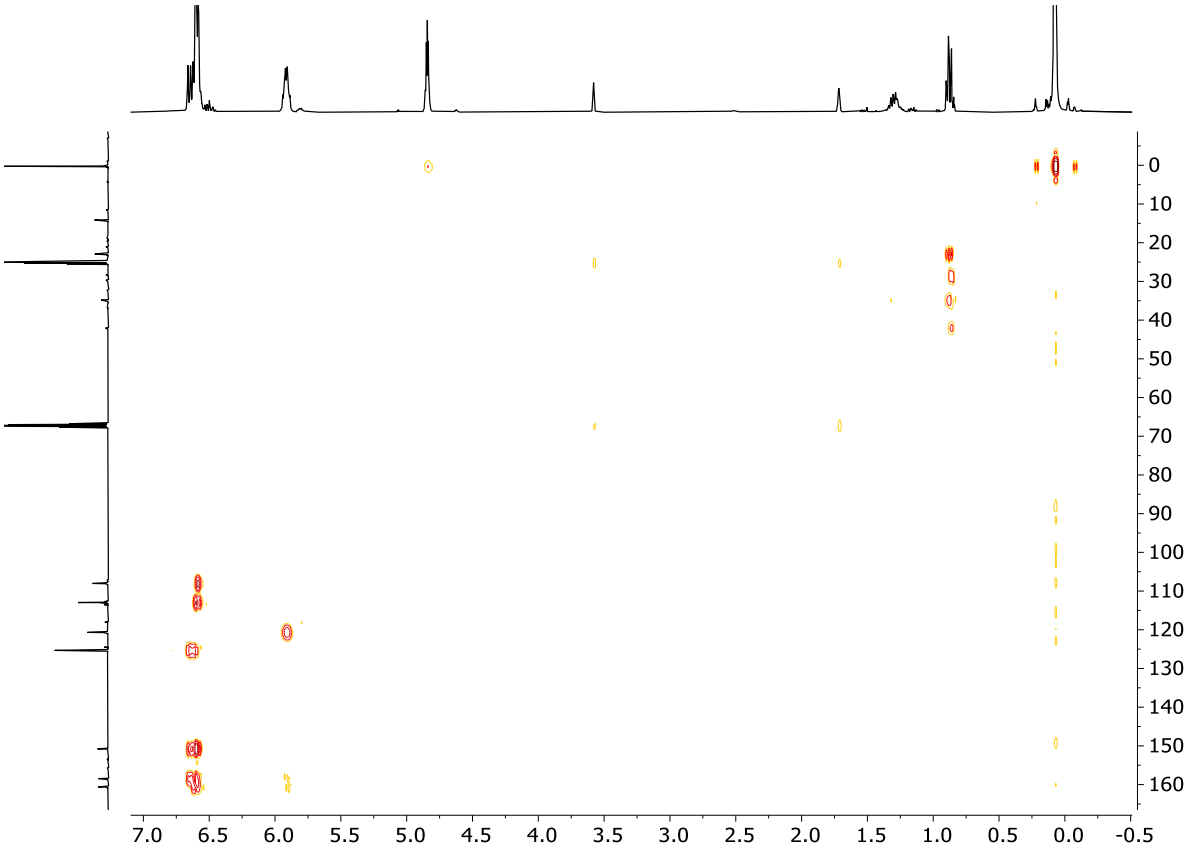

Fig. S40. HMBC ^{1}H-^{13}C NMR (benzene-d_6, 400.16/100.63 MHz, 27 °C) of *N*-(2-fluorophenyl)-dimethylsilylamide (**4-Li**).

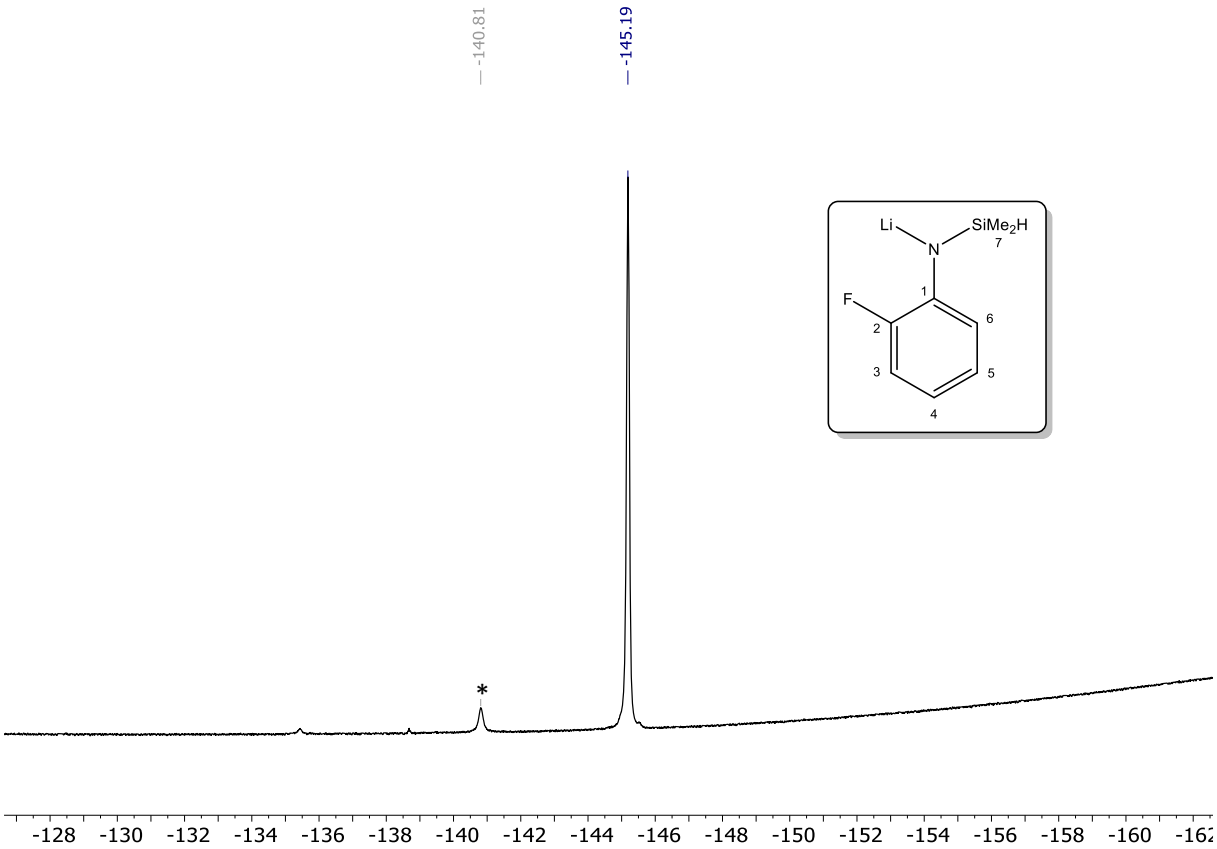

Fig. S41. ^{19}F NMR spectrum (thf-d_8, 376.44 MHz, 24 °C) of *N*-(2-fluorophenyl)-dimethylsilylamide (**4-Li**). The presence of a decomposition product (*) is rapidly visible and its concentration grows with time.

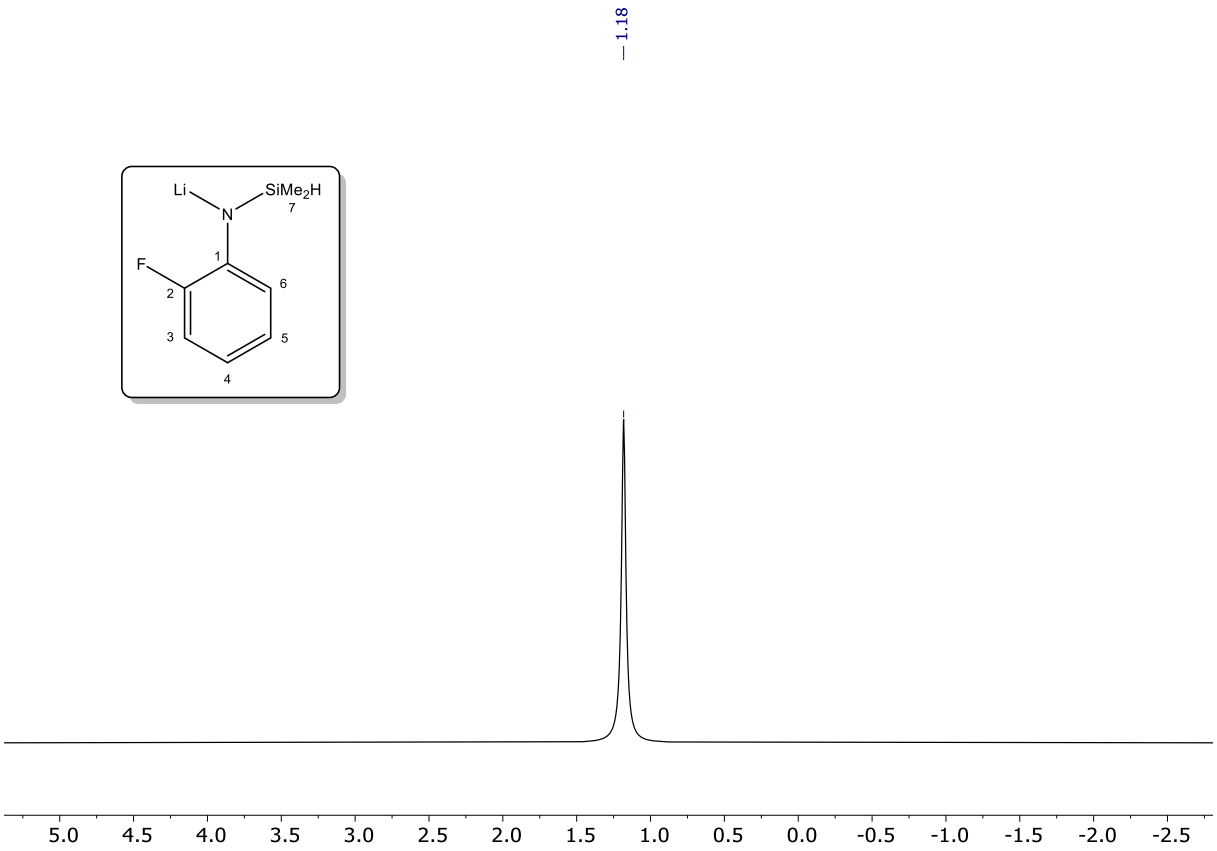

Fig. S42. ^{7}Li NMR spectrum (thf-d_8, 155.51 MHz, 24 °C) of *N*-(2-fluorophenyl)-dimethylsilylamide (**4-Li**).

X-ray diffraction crystallography details

	Complex identifier	Experiment number number	CCDC
lithium *N*-(2,6-difluorophenyl)-trimethylsilylamide	**[2-Li]$_\infty$**	PC_AAY	2238385
lithium *N*-(pentafluorophenyl)-trimethylsilylamide	**[3-Li.Et$_2$O]$_2$**	YA_LiNF$_5$	2238384
lithium *N*-(2-fluorophenyl)-1,1-dimethylsilylamide	**[4-Li]$_8$**	JL91	2238386

For **[2-Li]$_\infty$** ($C_9H_{12}F_2LiNSi$, M = 207.23 g.mol^{-1}). A suitable crystal for X-ray diffraction single crystal experiment (colourless stick, dimensions = 0.300 × 0.120 × 0.110 mm) was selected and mounted on the goniometer head of a APEXII Kappa-CCD (Bruker-AXS) diffractometer equipped with a CCD plate detector, using Mo-Kα radiation (λ = 0.71073 Å, graphite monochromator) at T = 150(2) K. The crystal structure has been described in monoclinic symmetry and $P2_1/n$ (I.T.#14) centric space group. Cell parameters have been refined as follows: a = 10.760(2), b = 6.5810(16), c = 14.522(3) Å, β = 91.476(11) °, V = 1028.0(4) Å^3. Number of formula unit Z is equal to 4 and calculated density d and absorption coefficient μ values are 1.339 g.cm^{-3} and 0.212 mm^{-1}, respectively. The crystal structure was solved by dual-space algorithm using SHELXT (Sheldrick, 2015a), and then refined with full-matrix least-squares methods based on F^2 (SHELXL; Sheldrick, 2015b). All non-Hydrogen atoms were refined with anisotropic atomic displacement parameters. H atoms were finally included in their calculated positions and treated as riding on their parent atom with constrained thermal parameters. A final refinement on F^2 with 2289 unique intensities and 130 parameters converged at ωR_{F2} = 0.1968 (R_F = 0.0834) for 1344 observed reflections with I > 2σ(I).

For **[3-Li.Et$_2$O]$_2$** ($C_{26}H_{38}F_{10}Li_2N_2O_2Si_2$, M = 670.64 g.mol^{-1}). A suitable crystal for X-ray diffraction single crystal experiment (colourless prism, dimensions = 0.600 × 0.490 × 0.250 mm) was selected and mounted on the goniometer head of a APEXII Kappa-CCD (Bruker-AXS) diffractometer equipped with a CCD plate detector, using Mo-Kα radiation (λ = 0.71073 Å, graphite monochromator) at T = 150(2) K. The crystal structure has been described in triclinic symmetry and P–1 (I.T.#2) centric space group. Cell parameters have been refined as follows: a = 9.0873(7), b = 10.5228(8), c = 10.6719(9) Å, α = 116.451(2), β = 99.726(3), γ = 106.944(2) °, V = 819.10(11) Å^3. Number of formula unit Z is equal to 1 and calculated density d and absorption coefficient μ values are 1.360 g.cm^{-3} and 0.191 mm^{-1}, respectively. The crystal structure was solved by dual-space algorithm using SHELXT (Sheldrick, 2015a), and then refined with full-matrix least-squares methods based on F^2 (SHELXL; Sheldrick, 2015b). All non-hydrogen atoms were refined with anisotropic atomic displacement parameters. H atoms were finally included in their calculated positions and treated as riding on their parent atom with constrained thermal parameters. A final refinement on F^2 with 3713 unique intensities and 204 parameters converged at ωR_{F2} = 0.1094 (R_F = 0.0389) for 3151 observed reflections with I > 2σ(I).

For **[4-Li]$_8$** ($C_{64}H_{88}F_8Li_8N_8Si_8.C_7H_8$, M = 1493.79 g.mol^{-1}). D8 VENTURE Bruker AXS diffractometer equipped with a (CMOS) PHOTON 100 detector, Mo-Kα radiation (λ = 0.71073 Å, multilayer monochromator), T = 150 K; monoclinic *P*2/n (I.T.#13), a = 16.620(3), b = 12.903(2), c = 19.799(4) Å, β = 89.952(7) °, V = 4245.6(13) Å^3. Z = 2, d = 1.168 g.cm^{-3}, μ = 0.186 mm^{-1}. The structure was solved by dual-space algorithm using the SHELXT program (Sheldrick, 2015a), and then refined with full-matrix least-squares methods based on F^2 (SHELXL; Sheldrick, 2015b). All non-hydrogen atoms were refined with anisotropic atomic displacement parameters. Except hydrogen atoms linked to silicon atoms that were introduced in the structural model through Fourier difference maps analysis, H atoms were finally included in their calculated positions and treated as riding on their parent atom with constrained

thermal parameters. A final refinement on F^2 with 9756 unique intensities and 479 parameters converged at ωR_{F2} = 0.1227 (R_F = 0.0527) for 8734 observed reflections with $I > 2\sigma(I)$.